Supplementary Information for

"Defective N-Glycosylation of IL6 Induces Metastasis and Tyrosine Kinase Inhibitor Resistance in Lung Cancer"

Supplementary Figure Titles

Supplementary Fig. 1 *In Silico* Prediction of N-Glycosylation Sequons in the Human IL6 Protein Sequence.

Position	Residue	Score	Prediction
2	NSF	-0.76837183	Non-glycosylated
73	**NKS**	**0.74945274**	**Potential Glycosylated**
76	NMC	-0.99857155	Non-glycosylated
88	NNL	-0.90419002	Non-glycosylated
89	NLN	-0.89130303	Non-glycosylated
91	NLP	-0.84612492	Non-glycosylated
107	NEE	-1.0721104	Non-glycosylated
131	NRF	-0.92744557	Non-glycosylated
160	NLD	-0.6123683	Non-glycosylated
172	**NAS**	**0.9827567**	**Potential Glycosylated**
183	NQW	-0.93842914	Non-glycosylated

SeqName	Position	Potential	Jury	N-Glyc	Agreement result
NP_000591.1	73	NKSN	0.6159	(9/9)	++
NP_000591.1	172	NASL	0.3900	(6/9)	-

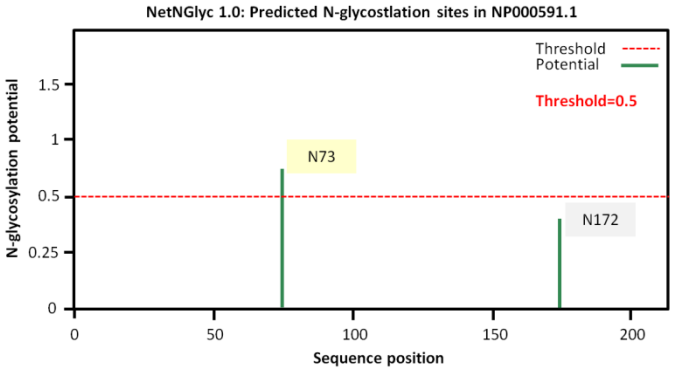

Supplementary Fig. 1 *In Silico* Prediction of N-Glycosylation Sequons in the Human IL6 Protein Sequence.
The N-glycosylation sites in the IL6 protein sequence were predicted with the NetNGlyc 1.0 server (http://www.cbs.dtu.dk/services/NetNGlyc/output.php). Two residues—N73 and N172—were identified as potential N-glycosites (upper panel). N73 met the default threshold criterion of a score of 0.5 (lower panel), whereas the score for N172 was lower than the threshold.

Supplementary Fig. 2 Demonstration of Predicted Glycosites on the Human IL6 Protein.

a

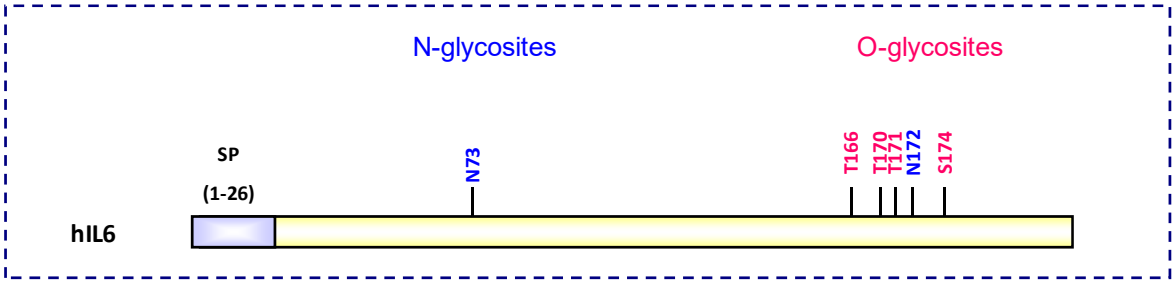

b

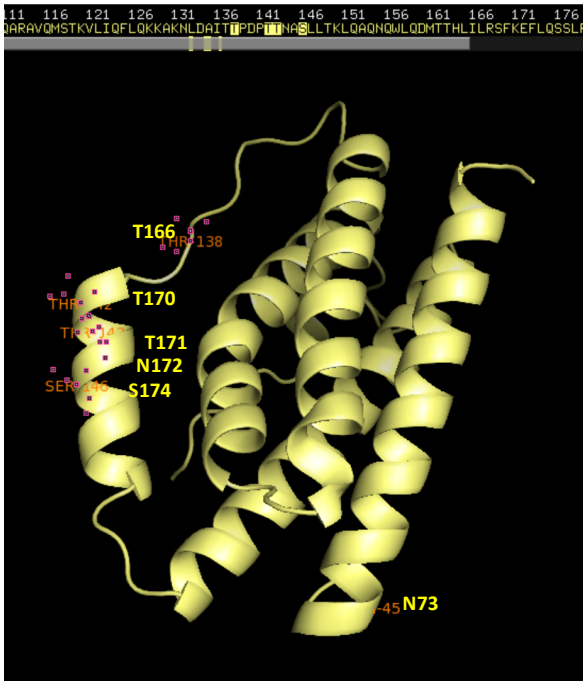

Supplementary Fig. 2 Demonstration of Predicted Glycosites on the Human IL6 Protein.

(a) N-glycosites and O-glycosites predicted in the hIL6 protein sequence.

(b) Three-dimensional representation of predicted N- and O-glycosites in the hIL6 protein by PyMOL.

Supplementary Fig. 3 Characterization of WT-IL6 from AS2-IL6-WT Cells.

a

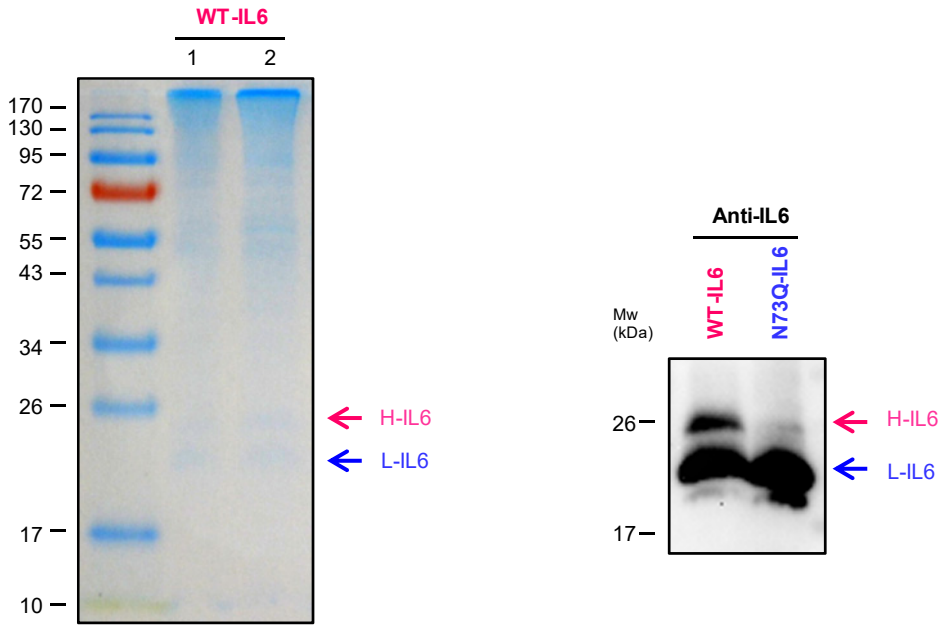

b

gi|23835 **Mass:** 20603 **Score:** 89 **Matches:** 6(3) **Sequences:** 5(3) **emPAI:** 0.67
26 kDa protein (aa 32-212) [Homo sapiens]
Check to include this hit in error tolerant search or archive report

Query	Observed	Mr(expt)	Mr(calc)	ppm	Miss	Score	Expect	Rank	Unique	Peptide
☑ 436	490.2649	978.5152	978.5134	1.80	0	19	3.4	1	U	K.EFLQSSLR.A
☑ 717	541.7406	1081.4667	1081.4676	-0.82	0	64	6.5e-005	1	U	R.FESSEEQAR.A
718	541.7503	1081.4861	1081.4676	17.1	0	(20)	1.9	3	U	R.FESSEEQAR.A
☑ 822	560.8220	1119.6295	1119.6288	0.65	0	41	0.012	1	U	R.YILDGISALR.K
☑ 1391	663.3561	1324.6976	1324.6986	-0.78	0	48	0.0052	1	U	K.EALAENNLNLPK.M
1950	1157.1331	2312.2516	2312.2587	-3.06	2	3	1e+002	8	U	K.KAKNLDAITTPDPTTNASLLTK.L

Proteins matching the same set of peptides:
gi|10834984 **Mass:** 23703 **Score:** 89 **Matches:** 6(3) **Sequences:** 5(3)
interleukin-6 precursor [Homo sapiens]
gi|33358027 **Mass:** 21065 **Score:** 89 **Matches:** 6(3) **Sequences:** 5(3)
Chain B, Crystal Structure Of The Hexameric Human Il-6IL-6 Alpha ReceptorGP130 COMPLEX
gi|157829952 **Mass:** 21099 **Score:** 89 **Matches:** 6(3) **Sequences:** 5(3)
Chain A, Human Interleukin-6
gi|157831463 **Mass:** 20968 **Score:** 89 **Matches:** 6(3) **Sequences:** 5(3)
Chain A, Human Interleukin-6, Nmr, Minimized Average Structure
gi|380861372 **Mass:** 23646 **Score:** 89 **Matches:** 6(3) **Sequences:** 5(3)
interleukin 6 [Homo sapiens]

H-IL6

gi|23835 **Mass:** 20603 **Score:** 151 **Matches:** 5(4) **Sequences:** 5(4) **emPAI:** 0.98
26 kDa protein (aa 32-212) [Homo sapiens]
Check to include this hit in error tolerant search or archive report

Query	Observed	Mr(expt)	Mr(calc)	ppm	Miss	Score	Expect	Rank	Unique	Peptide
☑ 454	490.2643	978.5141	978.5134	0.65	0	25	0.7	1	U	K.EFLQSSLR.A
☑ 484	494.8126	987.6106	987.6117	-1.08	0	61	3.9e-005	1	U	K.VLIQFLQK.K
☑ 728	541.7407	1081.4668	1081.4676	-0.69	0	65	5e-005	1	U	R.FESSEEQAR.A
☑ 833	560.8220	1119.6294	1119.6288	0.58	0	48	0.0026	1	U	R.YILDGISALR.K
☑ 1376	663.3561	1324.6977	1324.6986	-0.68	0	72	1.9e-005	1	U	K.EALAENNLNLPK.M

Proteins matching the same set of peptides:
gi|10834984 **Mass:** 23703 **Score:** 151 **Matches:** 5(4) **Sequences:** 5(4)
interleukin-6 precursor [Homo sapiens]
gi|33358027 **Mass:** 21065 **Score:** 151 **Matches:** 5(4) **Sequences:** 5(4)
Chain B, Crystal Structure Of The Hexameric Human Il-6IL-6 Alpha ReceptorGP130 COMPLEX
gi|157829952 **Mass:** 21099 **Score:** 151 **Matches:** 5(4) **Sequences:** 5(4)
Chain A, Human Interleukin-6
gi|157831463 **Mass:** 20968 **Score:** 151 **Matches:** 5(4) **Sequences:** 5(4)
Chain A, Human Interleukin-6, Nmr, Minimized Average Structure
gi|380861372 **Mass:** 23646 **Score:** 151 **Matches:** 5(4) **Sequences:** 5(4)
interleukin 6 [Homo sapiens]

L-IL6

Supplementary Fig. 3 Characterization of WT-IL6 from AS2-IL6-WT Cells.

(a) Affinity chromatography-purified WT-IL6 from AS2-IL6-WT cells was evaluated by SDS-PAGE with Coomassie blue staining (left) and by WB (right).

(b) MALDI-TOF characterization of purified WT-IL6 (H-IL6 and L-IL6).

Source data are provided as a Source Data file.

Supplementary Fig. 4 Establishment, Characterization, and Nomenclature of Various IL6 Glycoforms.

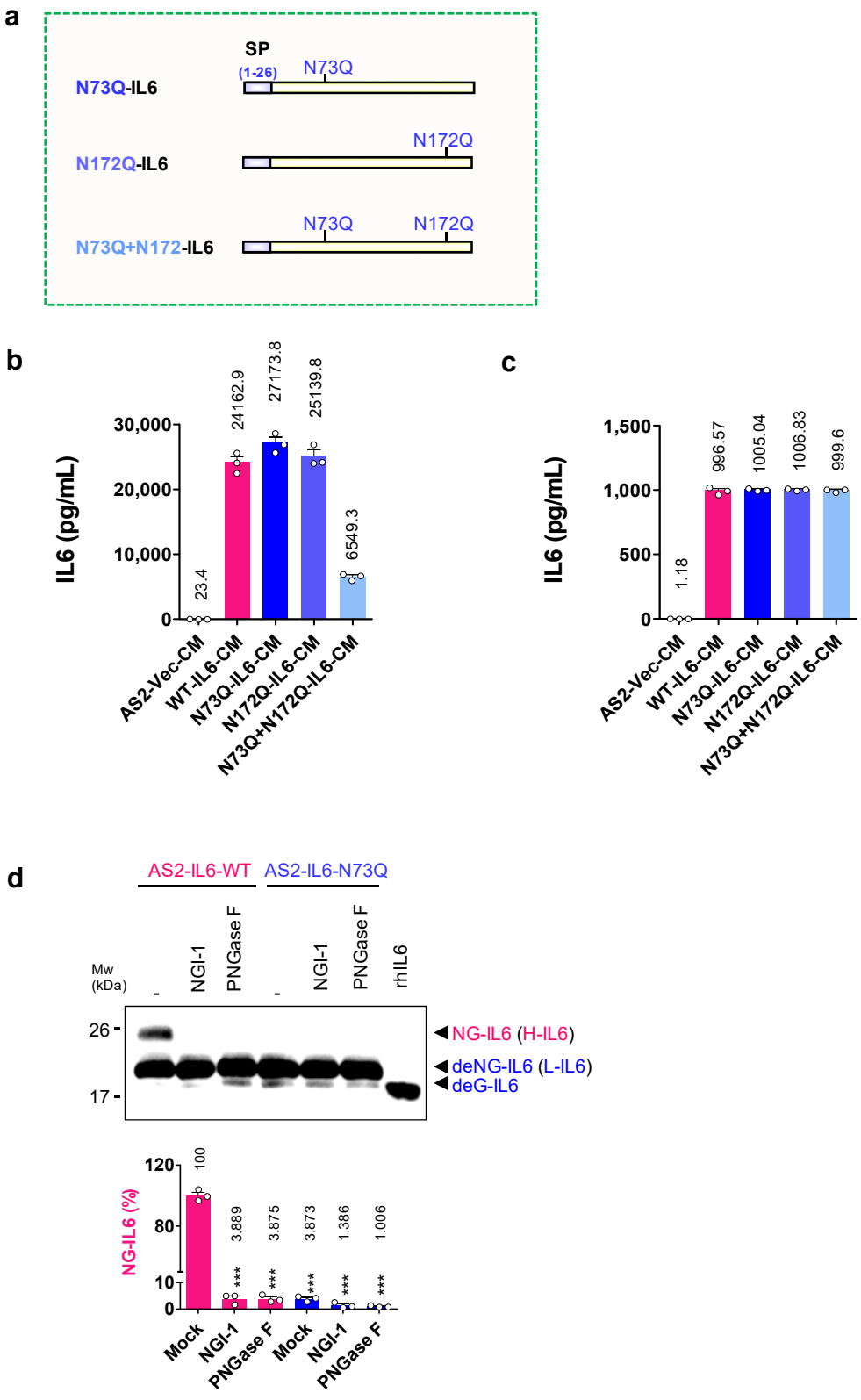

Supplementary Fig. 4 Establishment, Characterization, and Nomenclature of IL6 Glycoforms.

(a) Plasmid constructs of IL6 with various mutations in N-glycosites.

(b) IL6 concentrations in undiluted Vec-CM, WT-IL6-CM, N73Q-IL6-CM, N172Q-IL6-CM, and N73Q+N172Q- IL6-CM as measured by ELISA.

(c) IL6 concentrations in adjusted Vec-CM, WT-IL6-CM, N73Q-IL6-CM, N172Q-IL6-CM, and N73Q+N172Q- IL6-CM as measured by ELISA. The IL6 concentration was adjusted to 1 ng/mL with fresh MEM-α culture medium supplemented with 10% FBS, 1% anti-anti, 1% sodium pyruvate, and 5% MEM vitamin solution.

(d) Patterns of secreted IL6 from AS2-IL6-WT and AS2-IL6-N73Q cells with or without NGI-1 (10 μM) pretreatment for 48 h and of secreted IL6 with or without PNGase F digestion *in vitro*. n=3 independent experiments, mean ± SEM, two-tailed unpaired *t*-test. ***p<0.0001, ***p<0.0001, ***p<0.0001, ***p<0.0001, ***p<0.0001.

Source data are provided as a Source Data file.

Supplementary Fig. 5 Alignment of Full-Length hIL6 and Recombinant IL6 Generated by Bobby and Colleagues.

a

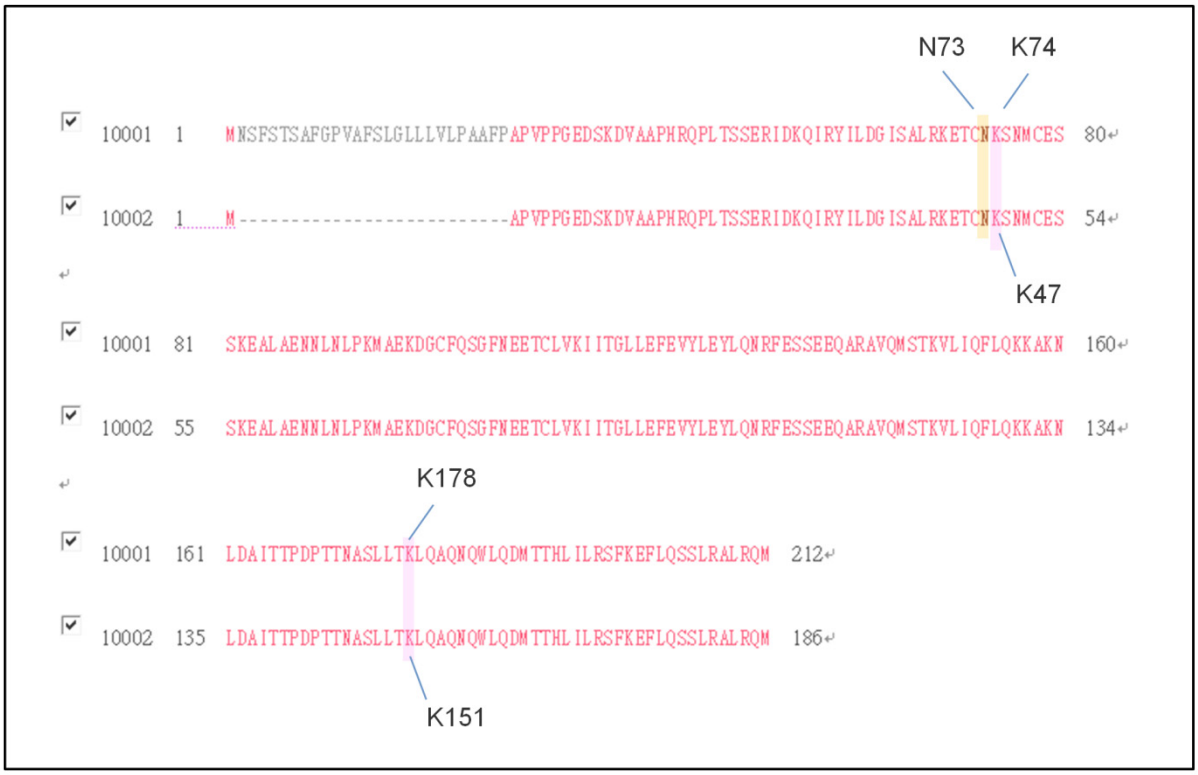

Peptide 10001: full-length hIL6 protein sequence from our construct
Peptide 10002: partial IL6 peptide sequence from Bobby *et.al.*

b

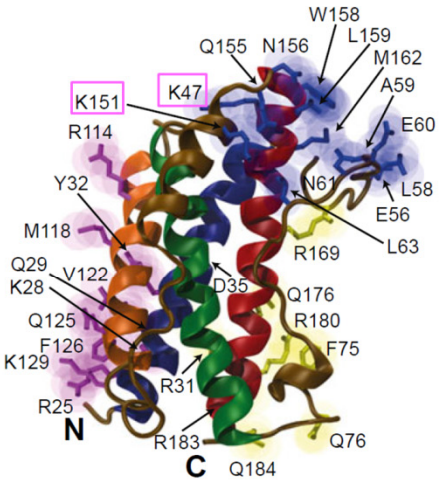

Supplementary Fig. 5 Alignment of Full-Length hIL6 and Recombinant IL6 Generated by Bobby and Colleagues.

The hIL6 protein sequence acquired from NCBI and the recombinant IL6 protein sequence generated by Bobby and colleagues (Bobby et al., 2014, doi:10.1111/febs.12800) were aligned by the Constraint-based Multiple Alignment Tool (COBAT) of NCBI. The yellow block indicates the N-glycosite at the N73 residue, and the magenta blocks indicate the two key lysine (K) residues stereochemically neighboring N73 and located in the IL6-GP130 interface.

Supplementary Fig. 6 Cytokines Contained in WT-IL6-CM and N73Q-IL6-CM.

a

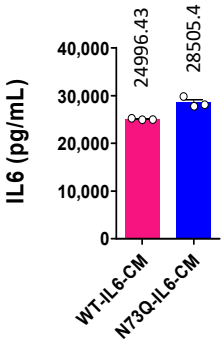

b

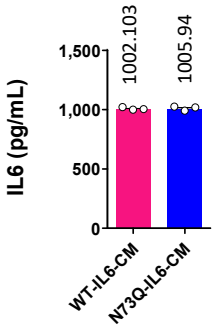

c

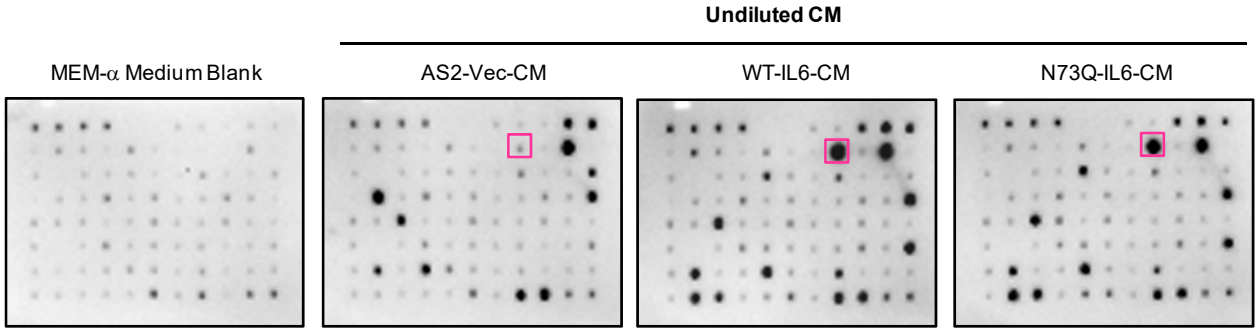

d

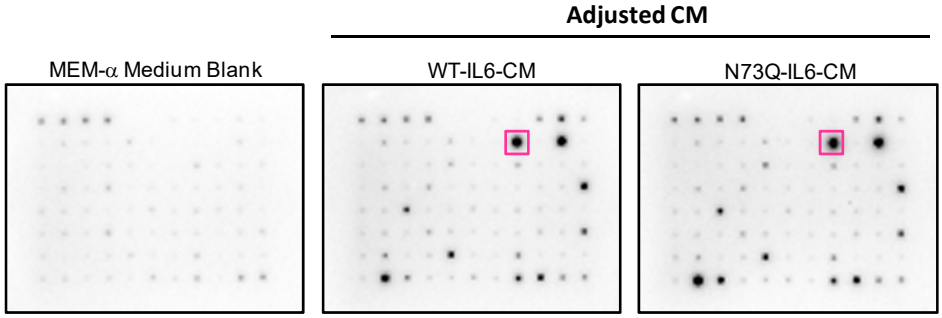

e

	A	B	C	D	E	F	G	H	I	J	K
1	POS	POS	POS	POS	NEG	NEG	ENA-78	G-CSF	GM-CSF	GRO	GRO alpha
2	I-309	IL-1 alpha	IL-1 beta	IL-2	IL-3	IL-4	IL-5	IL-6	IL-7	IL-8	IL-10
3	IL-12 p40/70	IL-13	IL-15	IFN gamma	MCP-1	MCP-2	MCP-3	M-CSF	MDC	MIG	MIP-1 beta
4	MIP-1 delta	RANTES	SCF	SDF-1	TARC	TGF beta 1	TNF alpha	TNF beta	EGF	IGF-1	ANG
5	OSM	THPO	VEGF	PDGF BB	Leptin	BDNF	BLC	CCL23	Eotaxin 1	Eotaxin 2	Eotaxin3
6	FGF 4	FGF 6	FGF 7	FGF 9	Flt-3 Ligand	Fractalkine	GCP-2	GDNF	HGF	IGFBP 1	IGFBP2
7	IGFBP 3	IGFBP 4	IL-16	IP-10	LIF	LIGHT	MCP-4	MIF	MIP-3 alpha	NAP-2	NT-3
8	NT-4	OPN	OPG	PARC	PLGF	TGF beta 2	TGF beta 3	TIMP-1	TIMP-2	POS	POS

Supplementary Fig. 6 Cytokines Contained in WT-IL6-CM and N73Q-IL6-CM.

(a) IL6 levels in undiluted WT-IL6-CM and N73Q-IL6-CM as measured by ELISA.

(b) IL6 levels in adjusted WT-IL6-CM and N73Q-IL6-CM as measured by ELISA. IL6 levels were adjusted to 1 ng/mL with fresh MEM-α culture medium supplemented with 10% FBS, 1% Anti-Anti, 1% sodium pyruvate, and 5% MEM vitamin solution.

(c) Cytokine arrays performed with undiluted CM.

(d) Cytokine arrays performed with adjusted CM. IL6 levels in WT-IL6-CM and N73Q-IL6-CM were measured by ELISAs and adjusted to 1 ng/mL with fresh MEM-α culture medium. One milliliter of the adjusted CM was incubated with a cytokine array overnight. The expression of cytokines was detected following the manufacturer's protocol.

(e) The cytokine array map.

Source data are provided as a Source Data file.

Supplementary Fig. 7 GP130 Blockade Reduced the WT-IL6-CM- and N73Q-IL6-CM-Induced Activation of STAT3.

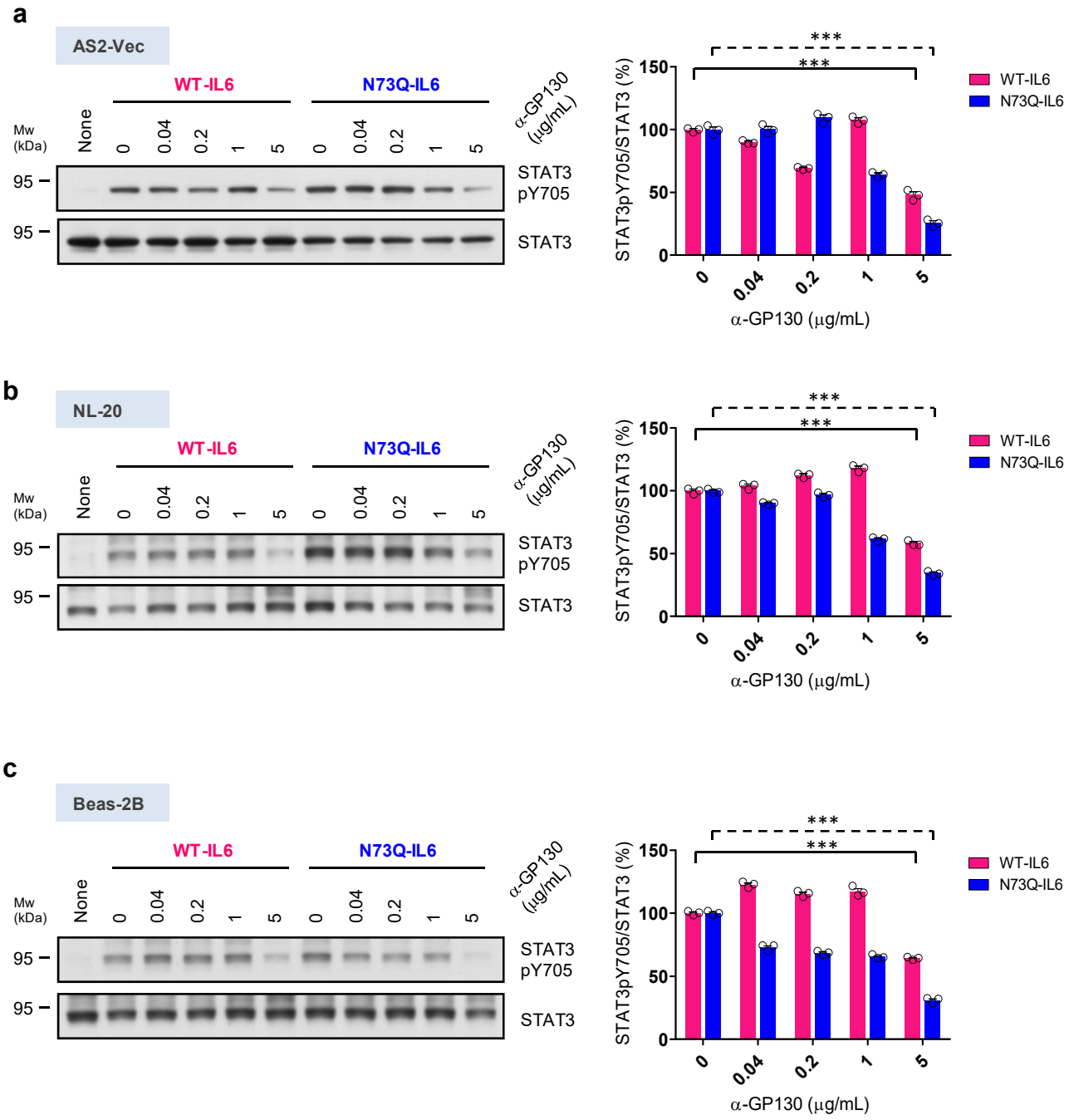

Supplementary Fig. 7 GP130 Blockade Reduced the WT-IL6-CM- and N73Q-IL6-CM-Induced Activation of STAT3.

AS2-Vec **(a)**, NL-20 **(b)**, and Beas-2B **(c)** cells were pretreated with GP130 neutralizing Ab at the indicated doses for 2 h followed by WT-IL6-CM- or N73Q-IL6-CM treatment for 0.5 h. STAT3pY705/STAT3 at GP130= 0 μg/mL was set as 100%, and STAT3pY705/STAT3 at each concentration was normalized to this value. n=3 independent experiments, mean ± SEM, two-tailed unpaired *t*-test. **(a)** WT-IL6-0 v.s. WT-IL6-5 ***p<0.0001, Q-0 v.s. Q-5 ***p<0.0001; **(b)** WT-IL6-0 v.s. WT-IL6-5 ***p<0.0001, Q-0 v.s. Q-5 ***p<0.0001; **(c)** WT-IL6-0 v.s. WT-IL6-5 ***p<0.0001, Q-0 v.s. Q-5 ***p<0.0001. Source data are provided as a Source Data file.

Supplementary Fig. 8 GP80 Blockade Reduced the WT-IL6-CM- and N73Q-IL6-CM-Induced Activation of STAT3.

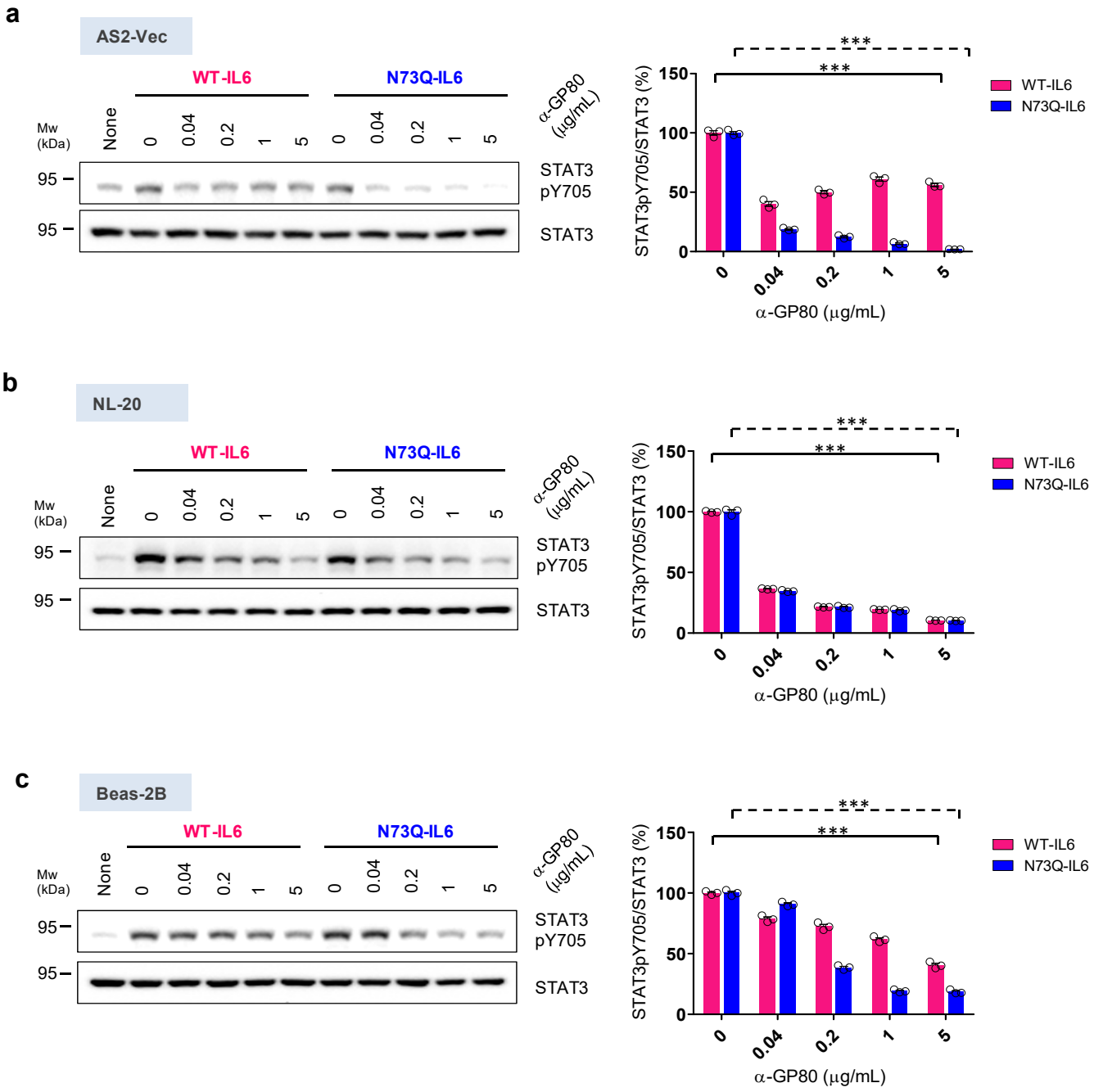

Supplementary Fig. 8 GP80 Blockade Reduced the WT-IL6-CM- and N73Q-IL6-CM-Induced Activation of STAT3. AS2-Vec **(a)**, NL-20 **(b)**, and Beas-2B **(c)** cells were pretreated with GP80 neutralizing Ab at the indicated doses for 2 h followed by WT-IL6-CM- or N73Q-IL6-CM treatment for 0.5 h. STAT3pY705/STAT3 at GP80= 0 μg/mL was set as 100%, and STAT3pY705/STAT3 at each concentration was normalized to this value. n=3 independent experiments, mean ± SEM, two-tailed unpaired *t*-test. **(a)** WT-IL6-0 v.s. WT-IL6-5 ***p<0.0001, Q-0 v.s. Q-5 ***p<0.0001; **(b)** WT-IL6-0 v.s. WT-IL6-5 ***p<0.0001, Q-0 v.s. Q-5 ***p<0.0001; **(c)** WT-IL6-0 v.s. WT-IL6-5 ***p<0.0001, Q-0 v.s. Q-5 ***p<0.0001. Source data are provided as a Source Data file.

Supplementary Fig. 9 IL6 Neutralization Reduced the WT-IL6-CM- and N73Q-IL6-CM-Induced Activation of STAT3.

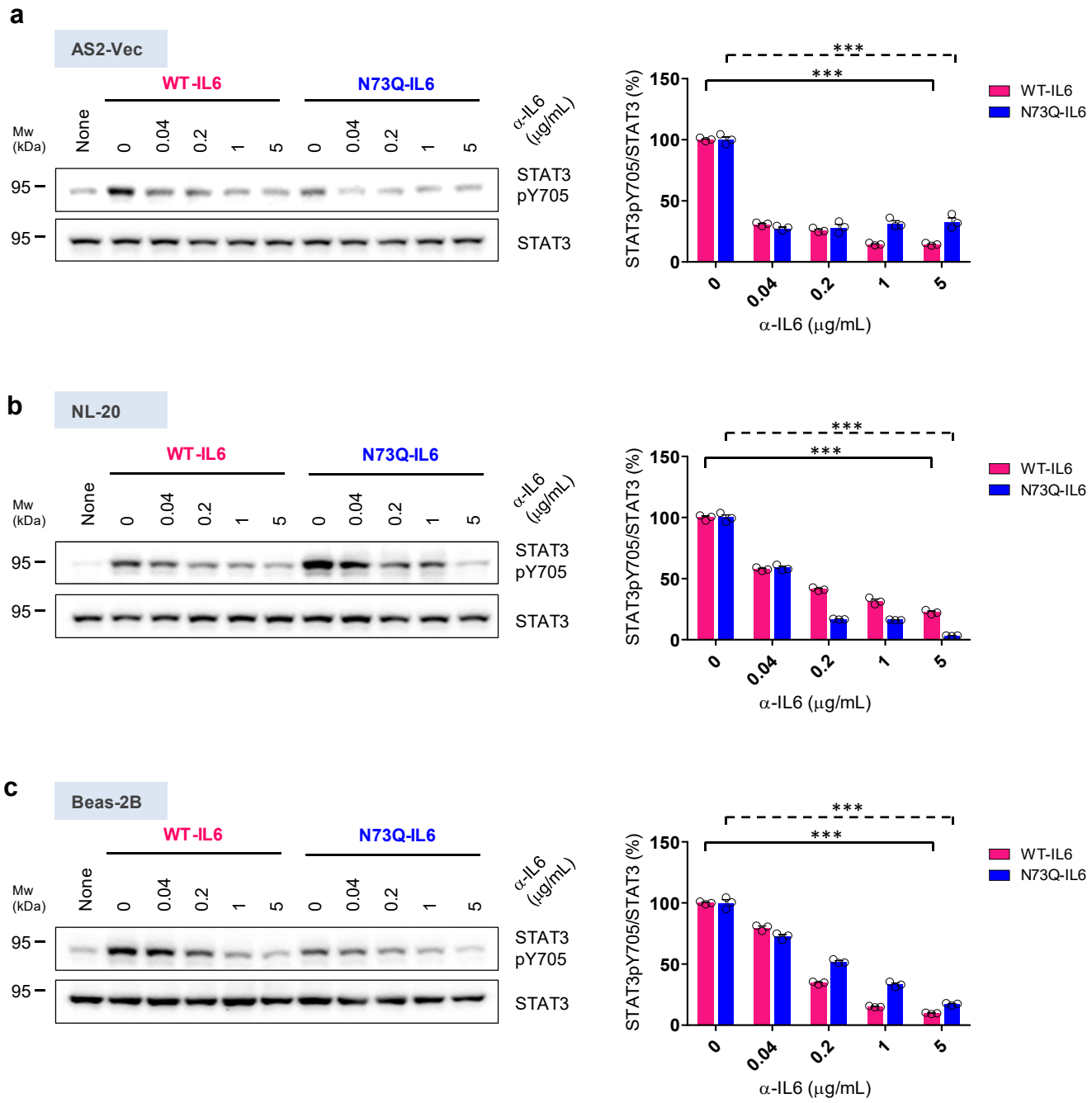

Supplementary Fig. 9 IL6 Neutralization reduced the WT-IL6-CM- and N73Q-IL6-CM-Induced Activation of STAT3.

WT-IL6-CM and N73Q-IL6-CM were preincubated with IL6 neutralizing Ab at indicated doses at 37 ℃ for 2 h. Then the AS2-Vec **(a)**, NL-20 **(b)**, and Beas-2B **(c)** cells were treated with the IL6-neutralized CM for 0.5 h. STAT3pY705/STAT3 at IL6 neutralizing Ab= 0 μg/mL was set as 100%, and STAT3pY705/STAT3 at eachconcentration was normalized to this value. n=3 independent experiments, mean ± SEM, two-tailed unpaired *t*-test. **(a)** WT-IL6-0 v.s. WT-IL6-5 ***p<0.0001, Q-0 v.s. Q-5 ***p<0.0001; **(b)** WT-IL6-0 v.s. WT-IL6-5 ***p<0.0001, Q-0 v.s. Q-5 ***p<0.0001; **(c)** WT-IL6-0 v.s. WT-IL6-5 ***p<0.0001, Q-0 v.s. Q-5 ***p<0.0001. Source data are provided as a Source Data file.

Supplementary Fig. 10 Hierarchical Clustering of Differentially Expressed Genes between WT-IL6-CM and N73Q-IL6-CM-Induced AS2-Vec Cells (>1.5 x FC) Over Time.

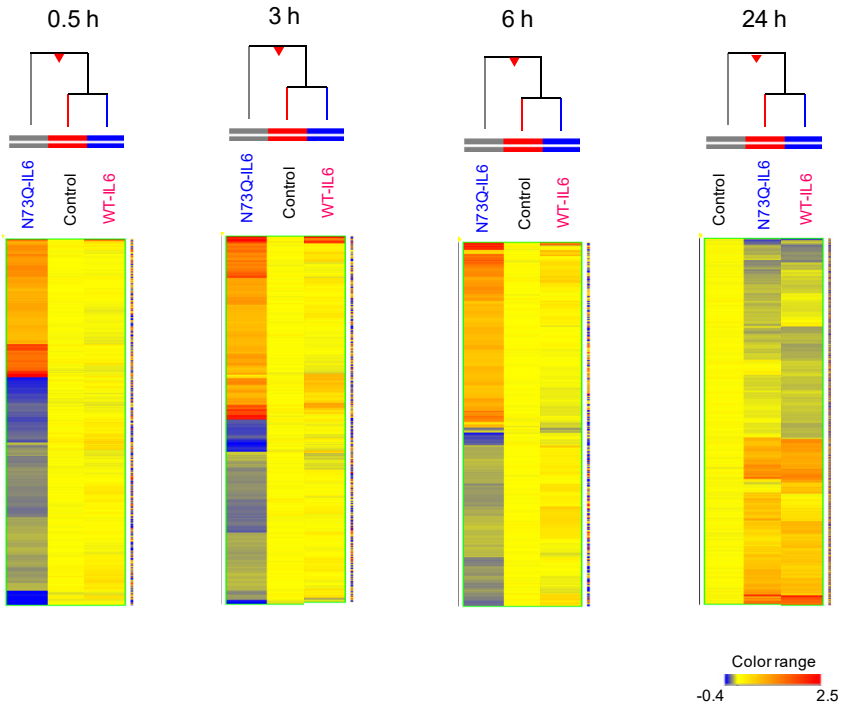

Supplementary Fig. 10 Hierarchical Clustering of Differentially Expressed Genes Between WT-IL6-CM- and N73Q-IL6-CM-Induced AS2-Vec Cells (FC >1.5) Over Time.

Transcriptomes of the AS2-Vec cells treated with WT-IL6-CM or N73Q-IL6-CM for the indicated durations. Differentially expressed mRNAs (fold change >1.5x) were hierarchically clustered with GeneSpring GX software.

Supplementary Fig. 11 Identification of Differentially Expressed Proteins in AS2-IL6-WT and AS2-IL6-N73Q Cells.

a

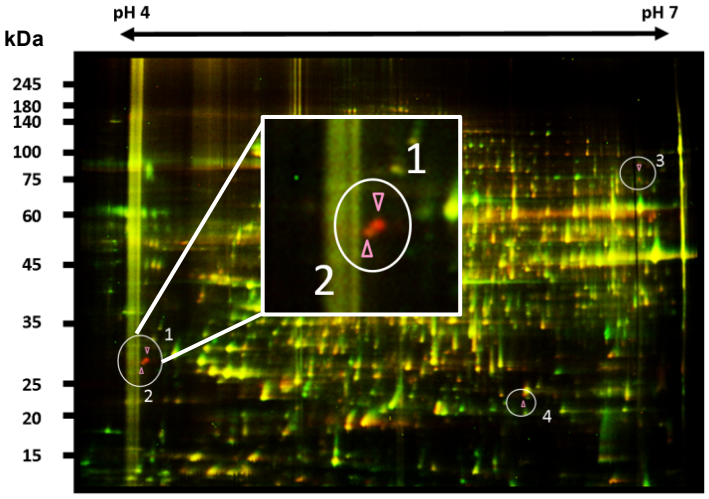

b

No.1
ANP32A, Acidic leucine-rich nuclear phosphoprotein 32 family member A
ANP32C, Acidic leucine-rich nuclear phosphoprotein 32 family member C
CMBP-4B, Charged multivesicular body protein 4b
EF1b2, Eukaryotic translation elongation factor 1 beta 2, isoform CRA_a
Filaggrin-2
HCG19809
Hepatopoietin PCn127
PRSS3 protein, Protease serine 3
No.2
ACTA1, Actin alpha 1 skeletal muscle protein
ACTA2, Actin, alpha 2, smooth muscle, aorta
Actin, cytoplasmic 2
CDNA FLJ52842, highly similar to Actin, cytoplasmic 1
Galectin-7
HCG15971, isoform CRA_a
PRSS3 protein, Protease serine 3
No.3
Caldesmon 1, isoform CRA_b
Epididymis secretory protein Li 105
Epididymis secretory sperm binding protein Li 94n
Ezrin
Far upstream element-binding protein 2
Polyribonucleotide nucleotidyltransferase 1, mitochondrial
Prelamin-A/C
PRSS1 protein, Protease serine 1
PRSS3 protein, Protease serine 3
Radixin
Stress-induced-phosphoprotein 1 (SIP-1)
TMPRSS13 protein, Transmembrane protease serine 13
No.4
Dermcidin
Epididymis secretory protein Li 102
Epididymis secretory sperm binding protein Li 128m
GrpE protein homolog 1, mitochondrial
Heat shock protein beta-1
Peroxiredoxin-6
PRSS1 protein, Protease serine 1
PRSS3 protein, Protease serine 3
TMPRSS13 protein, Transmembrane protease serine 13
Triosephosphate isomerase

Supplementary Fig. 11 Identification of Differentially Expressed Proteins in AS2-IL6-WT and AS2-IL6-N73Q Cells.

(a) Whole-cell lysates from the AS2-IL6-WT and AS2-IL6-N73Q cells were collected and labeled with Cy3 and Cy5, respectively. Proteins were separated by 2-dimensional gel electrophoresis, and images were acquired. Differentially expressed protein spots were identified by MultiGauge software and characterized by MALDI-TOF.

(b) Proteins in spots No. 1-4.

Supplementary Fig. 12 GP130 Blockade Suppressed the Formation of Stress Fibers in the N73Q-IL6-CM-Treated AS2-Vec Cells.

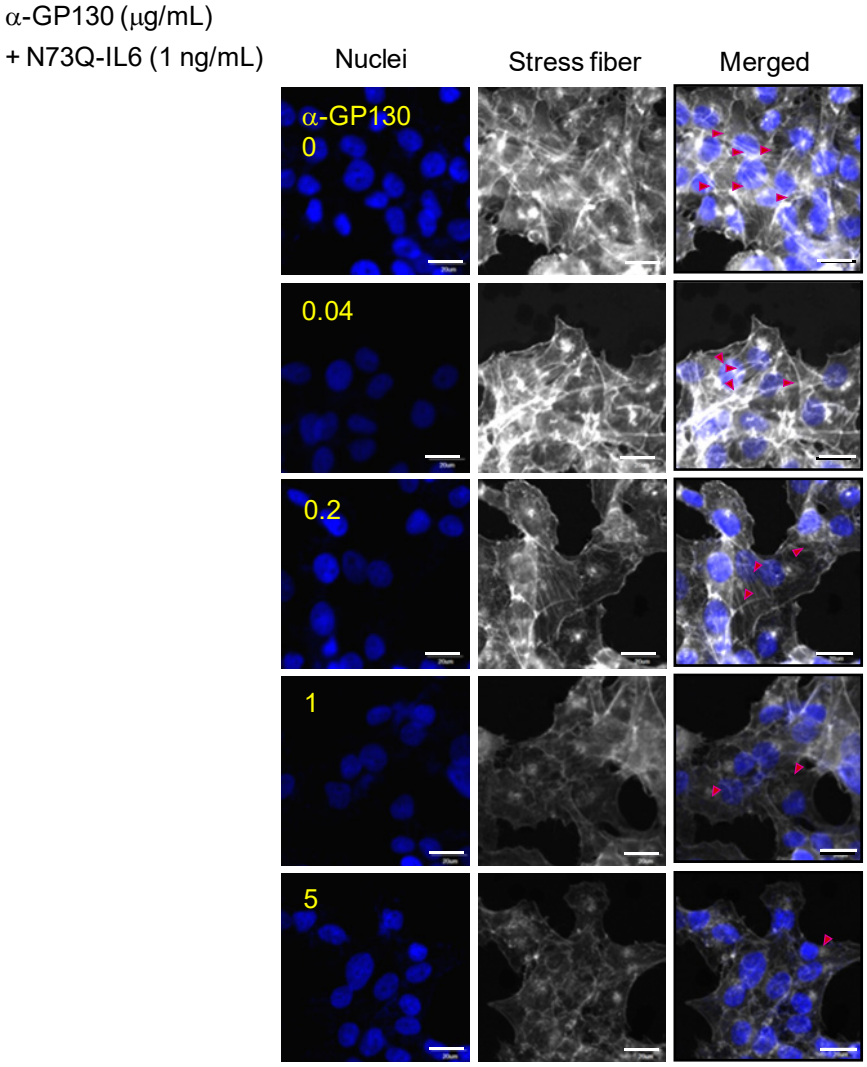

Supplementary Fig. 12 GP130 Blockade Suppressed the Formation of Stress Fibers in N73Q-IL6-CM-Treated AS2-Vec Cells.

Stress fibers in AS2-Vec cells under N73Q-IL6-CM treatment (24 h) with or without pretreatment with an α-GP130 neutralizing Ab at increasing concentrations for 2 h. Scale bars, 20 μm.

Supplementary Fig. 13 IL6 Signaling Blockade Suppressed the Expression of N73Q-IL6-CM-Induced Mesenchymal Proteins.

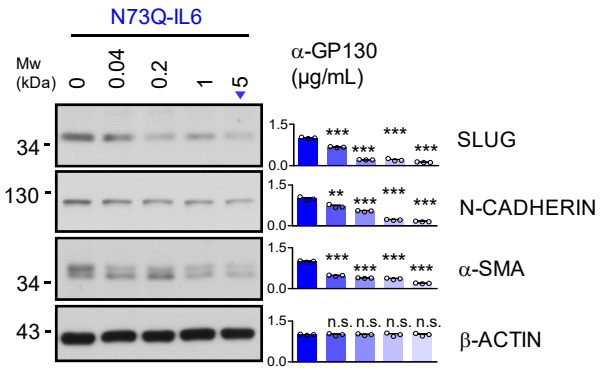

Supplementary Fig. 13 IL6 Signaling Blockade Suppressed the Expression of N73Q-IL6-CM-Induced Mesenchymal Proteins.

Expression of mesenchymal proteins in the AS2-Vec cells under N73Q-IL6-CM treatment (24 h) with or without α-GP130 neutralizing Ab pretreatment for 2 h. n=3 independent experiments, mean ± SEM, one-tailed unpaired *t*-test. SLUG: ***p<0.0001, ***p<0.0001, ***p<0.0001, ***p<0.0001; N-CADHERIN: **p=0.0034, ***p=0.0002, ***p<0.0001, ***p<0.0001; α-SMA: ***p=0.0001, ***p<0.0001, ***p<0.0001, ***p<0.0001; β-ACTIN: n.s. p=1.000, n.s. p=1.000, n.s. p=1.000, n.s. p=1.000. Source data are provided as a Source Data file.

Supplementary Fig. 14 Effects of Various N-Glycosylation-Defective IL6 Mutants on Migration.

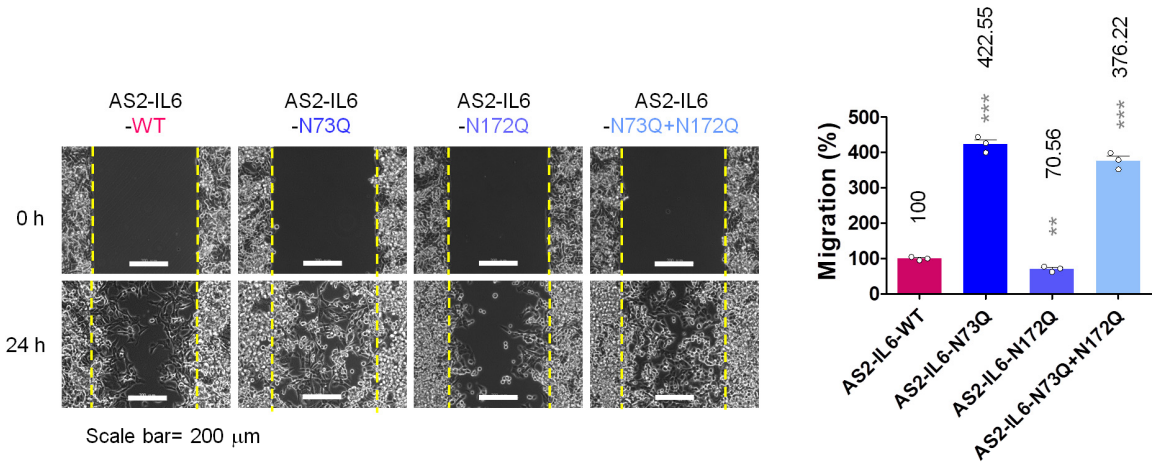

Supplementary Fig. 14 Effects of various N-glycosylation-defective IL6 mutants on migration.

The migration of AS2-IL6-WT, AS2-IL6-N73Q, AS2-IL6-N172Q, and AS2-IL6-N73Q+N172Q cells through the space made by culture inserts (upper images: 0 and 24 h). The medium contained mitomycin C (5 μg/mL). Scale bars, 200 μm. Quantitative results are presented next to the images. n=3 independent experiments, mean ± SEM, two-tailed unpaired *t*-test, ***p<0.0001, **p=0.0048, ***p<0.0001. Source data are provided as a Source Data file.

Supplementary Fig. 15 deNG-IL6 Enhances Metastatic Potential *In Vivo*.

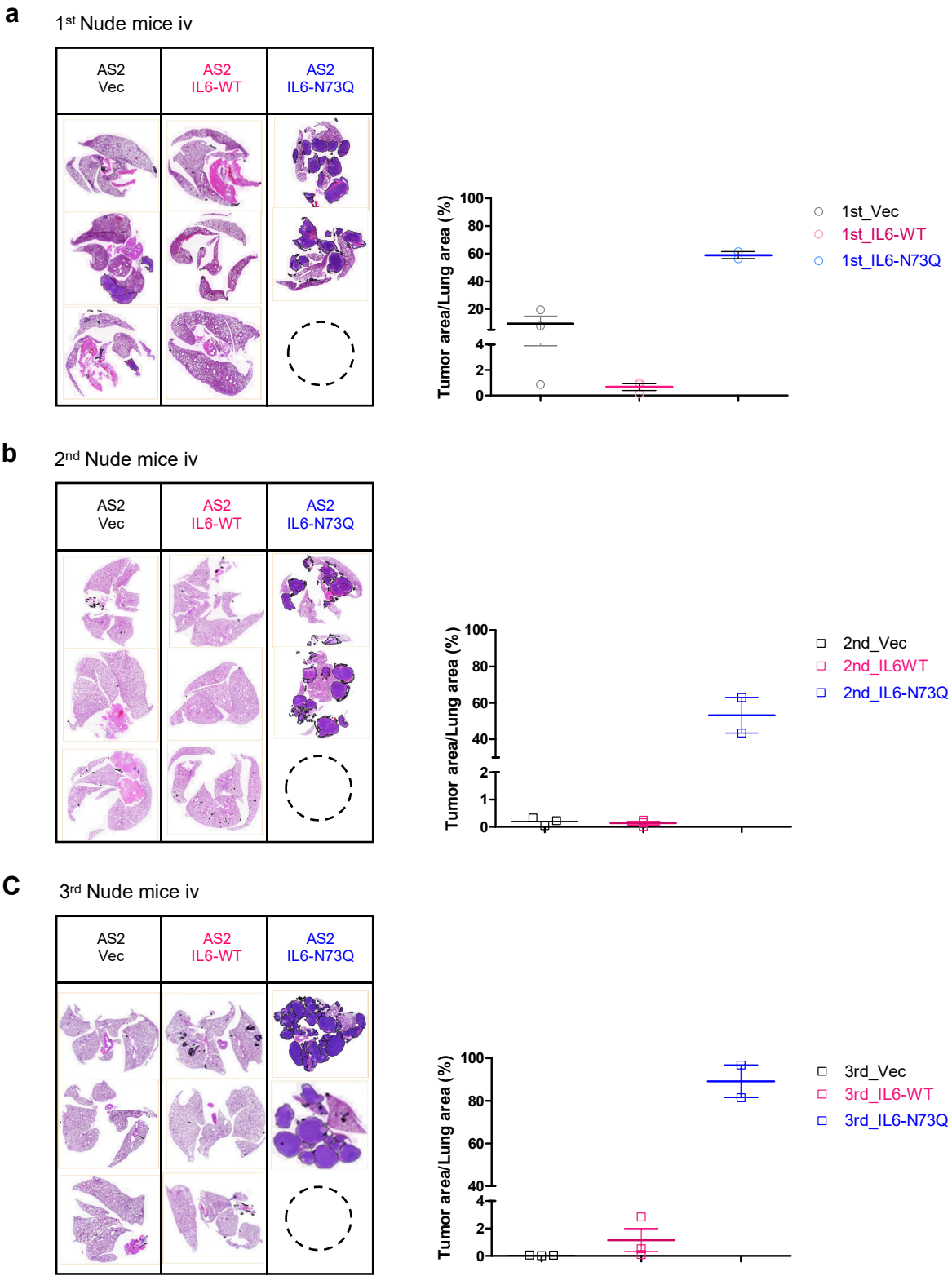

Supplementary Fig. 15 deNG-IL6 Enhanced the Metastatic Potential *In Vivo*.

In vivo metastasis of AS2-Vec, AS2-IL6-WT, and AS2-IL6-N73Q cells injected intravenously into nude mice (n=3 per cell type, 3 independent experimental replicates) evaluated by gross anatomical examination (left) and TissueFAXS-imaged H&E staining (right). The tumor area over the total lung area was quantified by HistoQuest. Each replicate experiment was terminated upon the death of the first animal. The necrotic lungs in these mice are indicated by dashed circles and were not used in further experiments. Source data are provided as a Source Data file.

Supplementary Fig. 16 Effect of Inhibitors against STAT3 or SRC Signaling on the Migration of AS2-Vec Cells.

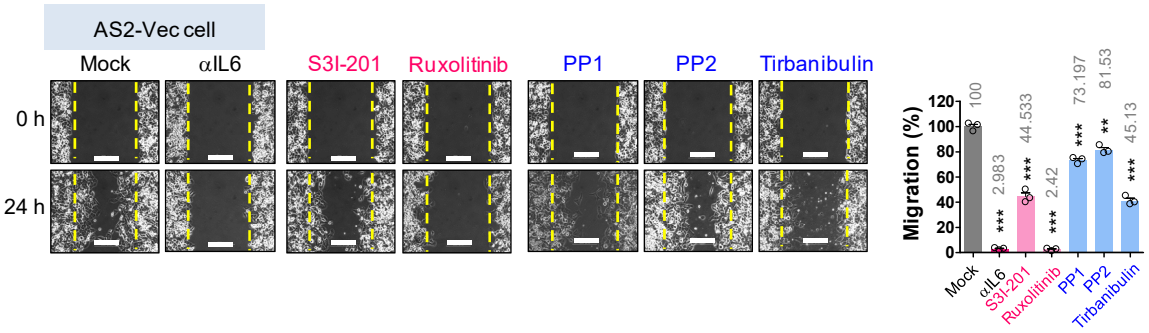

Supplementary Fig. 16 Effect of Inhibitors against STAT3 or SRC Signaling on the Migration of AS2-Vec Cells. Effect of IL6 neutralizing antibody (5 μg/mL), JAK-STAT3 inhibitors (S3I-201=10 μM, ruxolitinib=2.5 μM) and SRC inhibitors (PP1=10 μM, PP2=10 μM, tirbanibulin=10 μM) on the migration of AS2-IL6-WT and AS2-IL6-N73Q cells through the space made by culture inserts. The medium contained mitomycin C (5 μg/mL). Scale bars, 200 μm. Quantitative results are presented next to the images. n=3 independent experiments, mean ± SEM, one-tailed unpaired *t*-test, ***p<0.0001, ***p<0.0001, ***p<0.0001, ***p=0.0002, **p=0.0012, ***p<0.0001. Source data are provided as a Source Data file.

Supplementary Fig. 17 Effects of Various N-Glycosylation-Defective IL6 Mutants on JAK-STAT3 and SRC-YAP Signaling.

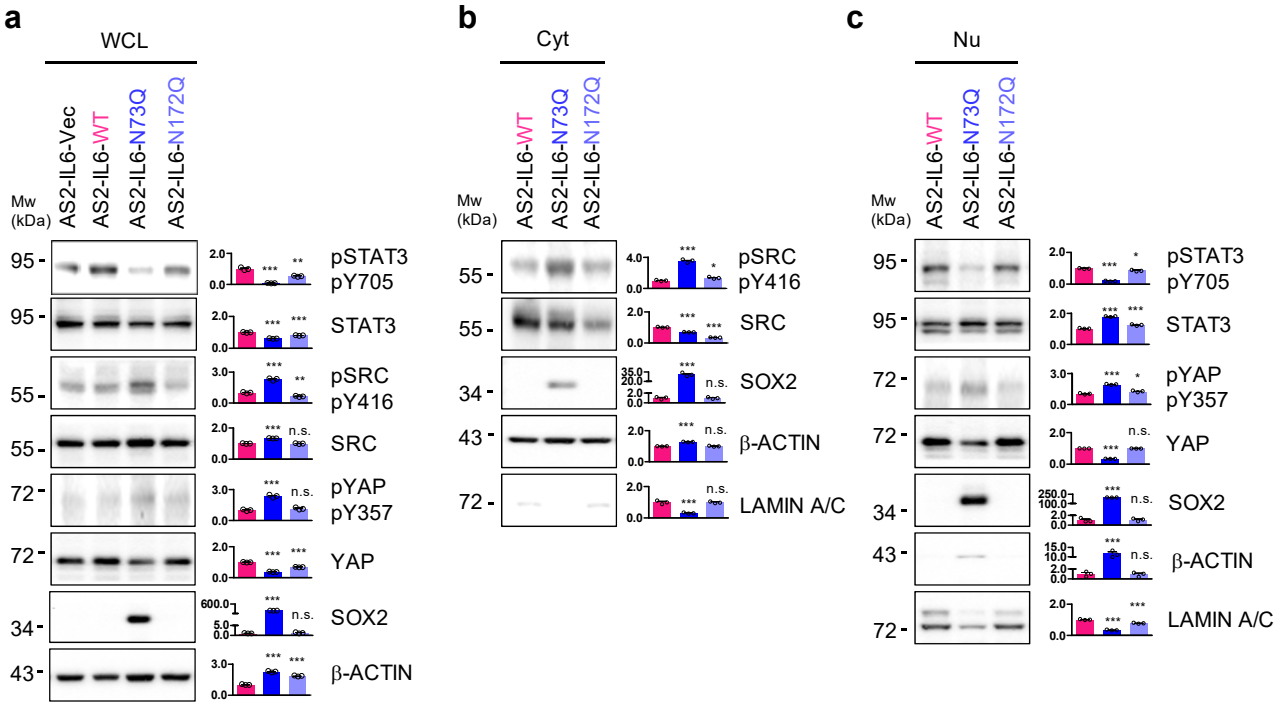

Supplementary Fig. 17 N-Glycosylation on N73 Residue is Responsible for Switching the GP130 Signaling Preference from the JAK-STAT3 Axis to the SRC-YAP Axis.

(a) Expression of proteins indicating the activation of STAT3, SRC, and YAP in AS2-Vec, AS2-IL6-WT, AS2-IL6-N73Q, and AS2-IL6-N172 cells. n=3 independent experiments, mean ± SEM, two-tailed unpaired *t*-test. STAT3pY705: ***p<0.0001, **p=0.0013; STAT3: ***p<0.0001, ***p=0.0005; SRCpY416: ***p<0.0001, **p=0.0019; SRC***p<0.0001, n.s. p=7964; YAPpY357: ***p=0.0001, n.s. p=0.1164; YAP: ***p<0.0001, ***p<0.0001; SOX2: ***p<0.0001, n.s. p=0.2897; β-ACTIN: ***p<0.0001, ***p<0.0001.

(b) Expression of proteins indicating the activation of STAT3 and SRC in the cytosolic fractions of the AS2-IL6-WT, AS2-IL6-N73Q, and AS2-IL6-N172Q cells. n=3 independent experiments, mean ± SEM, two-tailed unpaired *t*-test. SRCpY416: ***p<0.0001, *p=0.0144; SRC: ***p<0.0001, ***p<0.0001; SOX2:***p<0.0001, n.s. p=0.9943; β-ACTIN: ***p<0.0001, n.s. p=0.9071; LAMIN A/C: ***p=0.0006, n.s. p=1.0000.

(c) Expression of proteins indicating the activation of STAT3 and SRC in the nuclear fractions of the AS2-IL6-WT, AS2-IL6-N73Q, and AS2-IL6-N172Q cells. n=3 independent experiments, mean ± SEM, two-tailed unpaired *t*-test.

WCL: whole cell lysates; Cyt: cytosolic fraction; Nu: nuclear fraction. STAT3pY705: ***p<0.0001, *0.0100; STAT3:***p<0.0001, ***p<0.0001; YAPpY357:***p<0.0001, *p=0.0135; YAP: ***p<0.0001, n.s. p=0.3637; SOX2: ***p<0.0001, n.s. p=0.7812; β-ACTIN: ***p<0.0001, n.s. p=0.8338; LAMIN A/C: ***p<0.0001, ***p=0.0004. Source data are provided as a Source Data file.

Supplementary Fig. 18 N73A-IL6 and N73V-IL6 Demonstrated Biological Consequences Similar to N73Q-IL6.

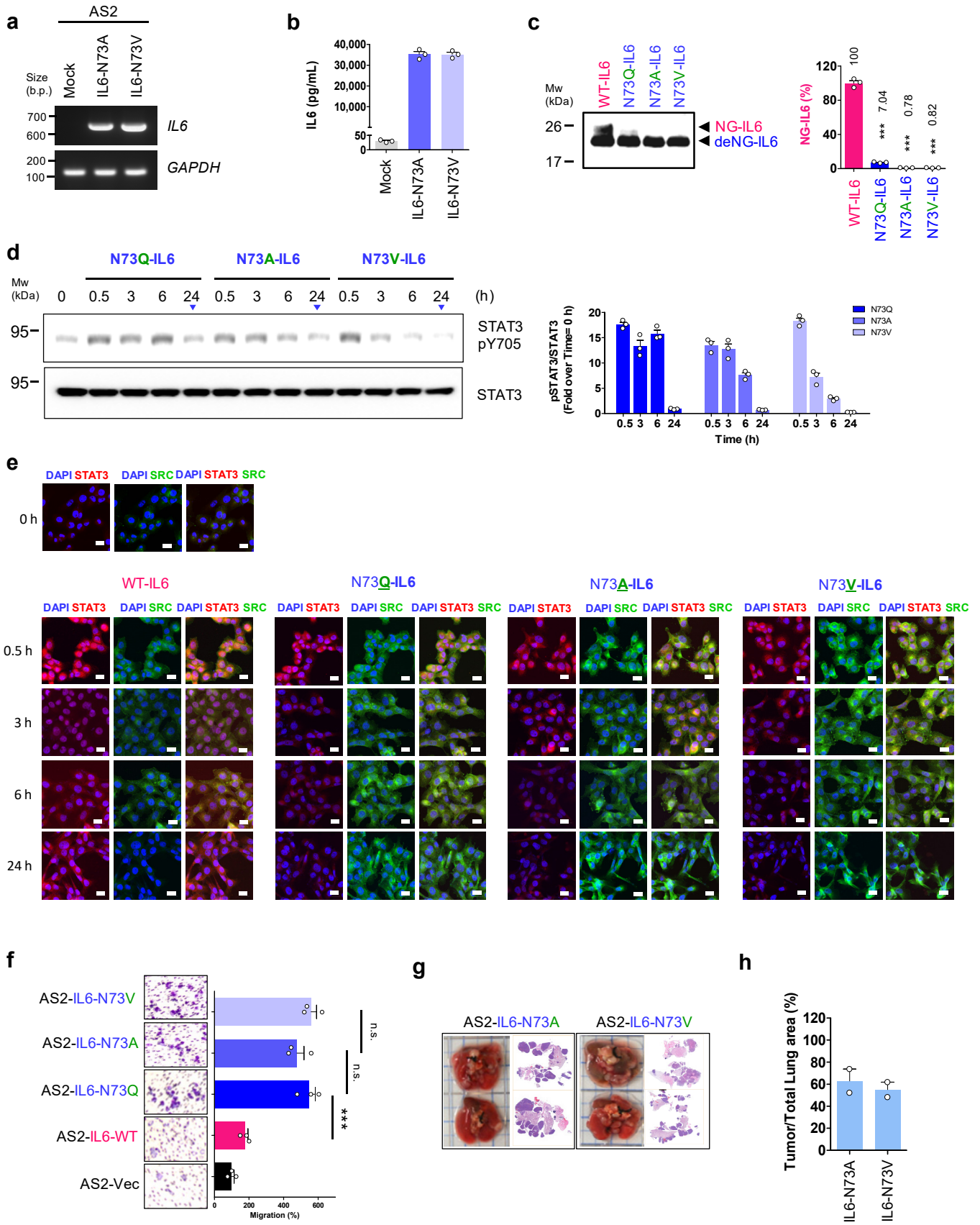

Supplementary Fig. 18 N73A-IL6 and N73V-IL6 Demonstrated Biological Consequences Similar to N73Q-IL6.

(a) *IL6* mRNA levels in AS2 cells stably expressing full-length N73A-hIL6 or N73V-hIL6 (namely, AS2-IL6-N73A and AS2-IL6-N73V cells), as measured by RT–PCR. *GAPDH* was the internal control.

(b) Quantity of total secreted IL6 in NSCLC cell lines as measured by ELISAs. n=3 technical replicates, mean ± SEM.

(c) Patterns of purified fully glycosylated WT-IL6 and deNG-IL6 (N73Q-IL6, N73A-IL6, N73V-IL6) secreted by AS2-IL6-WT, AS2-IL6-N73Q, AS2-IL6-N73A, and AS2-IL6-N73V cells. n=3 independent experiments, mean ± SEM, two-tailed unpaired *t*-test, ***p<0.0001, ***p<0.0001, ***p<0.0001.

(d) STAT3 and STAT3-pY705 levels induced by N73Q-IL6-CM, N73A-IL6-CM, or N73V-IL6-CM (IL6=1 ng/mL) over time in AS2-Vec cells (triplicate, mean ± SEM, *t*-test).

(e) Intracellular localization of STAT3 and SRC in AS2-Vec cells under treatment with WT-IL6-CM, N73Q-IL6-CM, N73A-IL6-CM, or N73V-IL6-CM (IL6=1 ng/mL) over time, as determined by IF (triplicate, mean ± SEM, *t*-test). The magnified insets show STAT3 localization at 24 h. Scale bars, 20 μm.

(f) Migration of AS2-Vec, AS2-IL6-WT, AS2-IL6-N73Q, AS2-IL6-N73A, and AS2-IL6-N73V cells through Transwell membranes n=3 independent experiments, mean ± SEM, two-tailed unpaired *t*-test. WT v.s. N73Q: ***p=0.0007; N73Q v.s. N73A: n.s. p=0.2768; N73A v.s. N73V: n.s. p=0.1925.

(g) *In vivo* metastasis of AS2-IL6-N73A and AS2-IL6-N73V cells injected intravenously into nude mice (n=2 per cell type) evaluated by gross anatomical examination (left) and TissueFAXS-imaged H&E staining (right).

(h) The tumor area over the total lung area from **(h)**, as quantified by HistoQuest (mean ± SEM).

Source data are provided as a Source Data file.

Supplementary Fig. 19 Cytokines Contained in CM of Parental and Osimertinib-Resistant PC9 and HCC827 Cells.

a

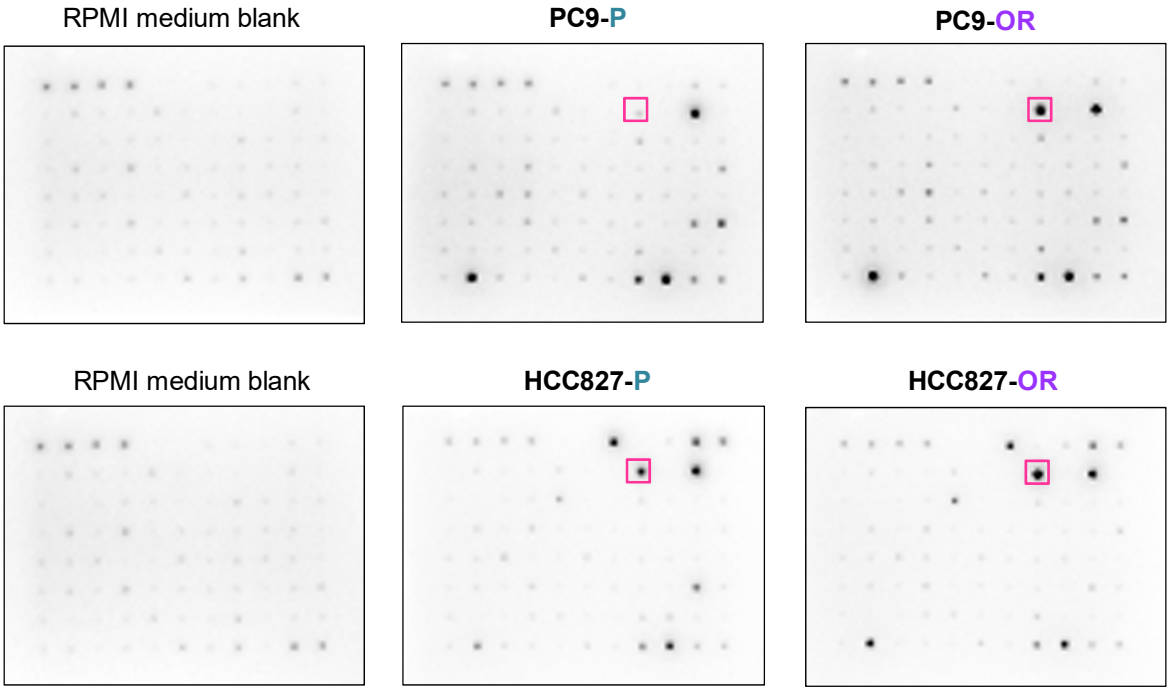

b

	A	B	C	D	E	F	G	H	I	J	K
1	POS	POS	POS	POS	NEG	NEG	ENA-78	G-CSF	GM-CSF	GRO	GRO alpha
2	I-309	IL-1 alpha	IL-1 beta	IL-2	IL-3	IL-4	IL-5	IL-6	IL-7	IL-8	IL-10
3	IL-12 p40/70	IL-13	IL-15	IFN gamma	MCP-1	MCP-2	MCP-3	M-CSF	MDC	MIG	MIP-1 beta
4	MIP-1 delta	RANTES	SCF	SDF-1	TARC	TGF beta 1	TNF alpha	TNF beta	EGF	IGF-1	ANG
5	OSM	THPO	VEGF	PDGF BB	Leptin	BDNF	BLC	CCL23	Eotaxin 1	Eotaxin 2	Eotaxin3
6	FGF 4	FGF 6	FGF 7	FGF 9	Flt-3 Ligand	Fractalkine	GCP-2	GDNF	HGF	IGFBP 1	IGFBP2
7	IGFBP 3	IGFBP 4	IL-16	IP-10	LIF	LIGHT	MCP-4	MIF	MIP-3 alpha	NAP-2	NT-3
8	NT-4	OPN	OPG	PARC	PLGF	TGF beta 2	TGF beta 3	TIMP-1	TIMP-2	POS	POS

Supplementary Fig. 19 Cytokines Contained in CM of Parental and Osimertinib-Resistant PC9 and HCC827 Cells.

(a) One milliliter of the undiluted CM was incubated with a cytokine array overnight. The expression of cytokines was detected following the manufacturer's protocol.

(b) The cytokine array map.

Supplementary Fig. 20 IL6 Neutralization Partially Restores Sensitivity to Osimertinib of Osimertinib-Resistant NSCLC Cells.

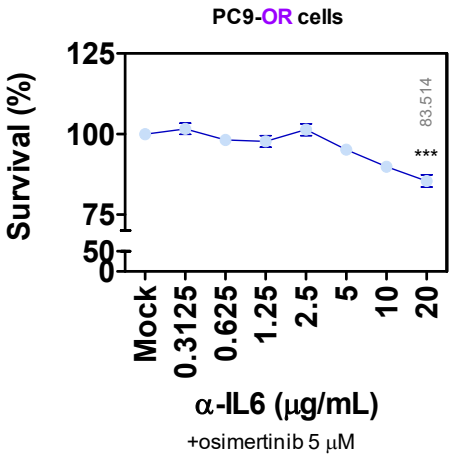

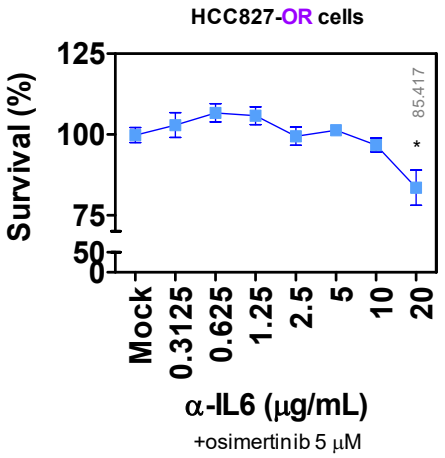

Supplementary Fig. 20 IL6 Neutralization Partially Restores Sensitivity to Osimertinib of Osimertinib-Resistant NSCLC Cells.

PC9-OR and HCC827-OR cells were maintained in medium containing resistance-tolerant osimertinib (5 mM) and treated with a neutralizing Ab against IL6 at the indicated doses. The survival of the cells was measured by MTT assay at 72 h. n=4 technical replicate, mean ± SEM, *o*ne-tailed unpaired *t*-test. PC9-OR: ***p=0.0005; HCC827-OR: * p=0.0164. Source data are provided as a Source Data file.

Supplementary Fig. 21 Relative Expression of N-Glycosylation-, EMT-, and SRC-YAP Pathway-Related Gene Sets.

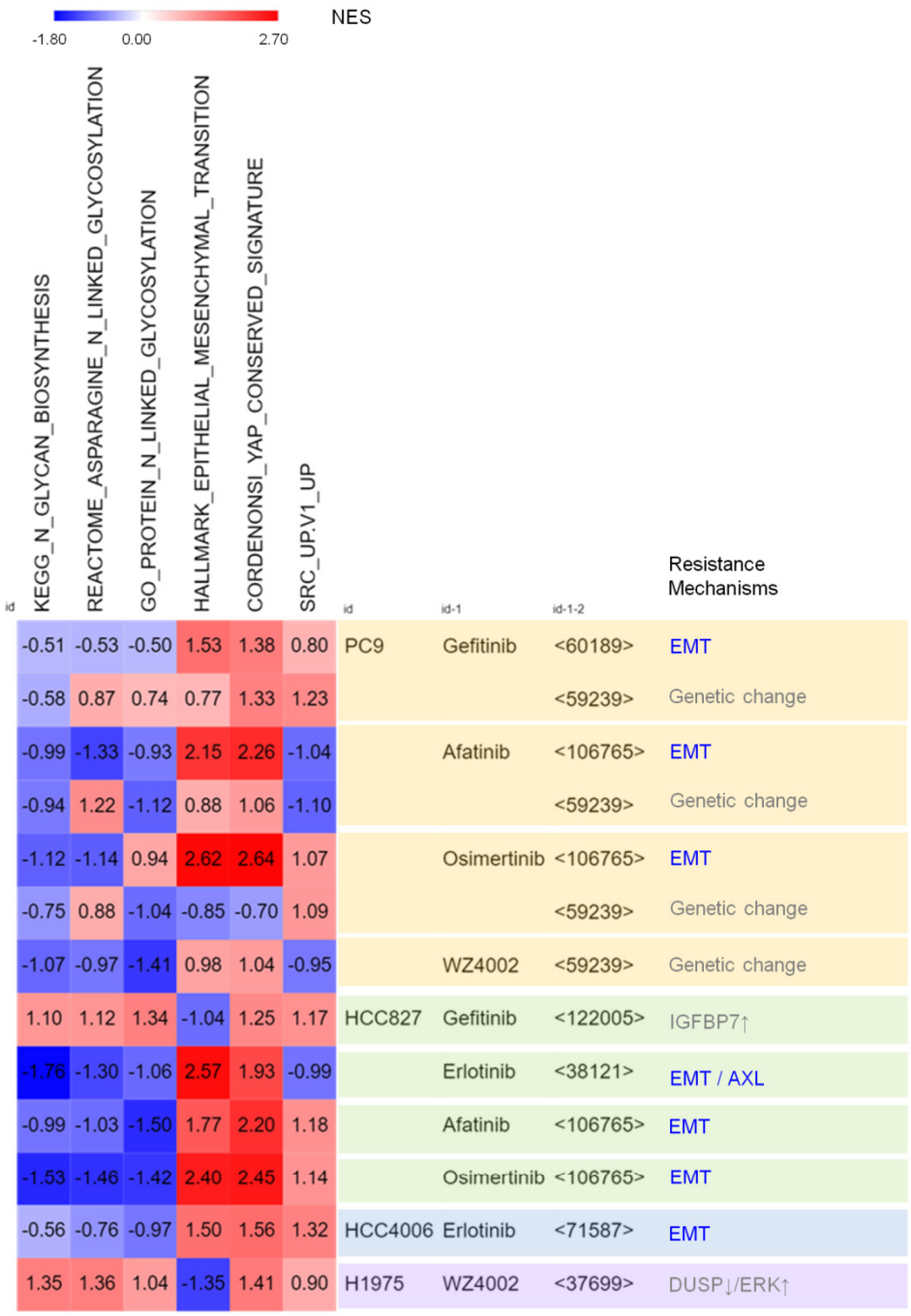

Supplementary Fig. 21 Relative Expression of N-Glycosylation-, EMT-, and SRC-YAP Pathway-Related Gene Sets.

Heatmap of enrichment scores for gene sets related to the N-glycosylation process, EMT, and SRC-YAP pathway in GSEA datasets containing data upon treatment with different EGFR-TKIs.

Supplementary Fig. 22 Identification of IL6 glycopeptides.

a

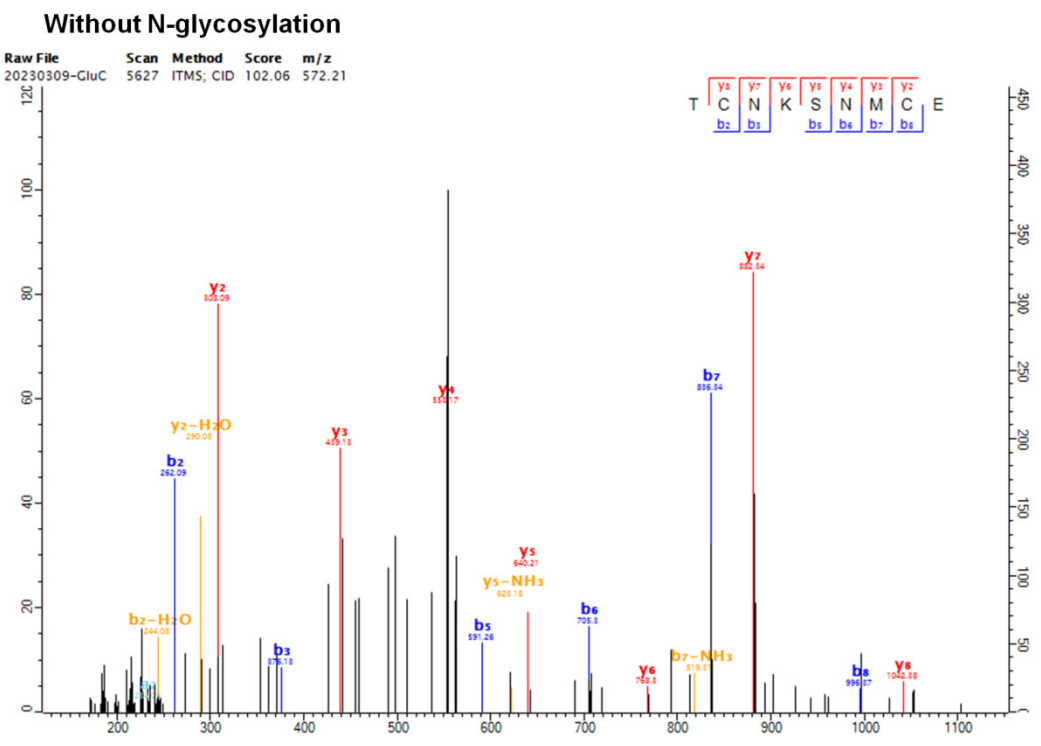

b

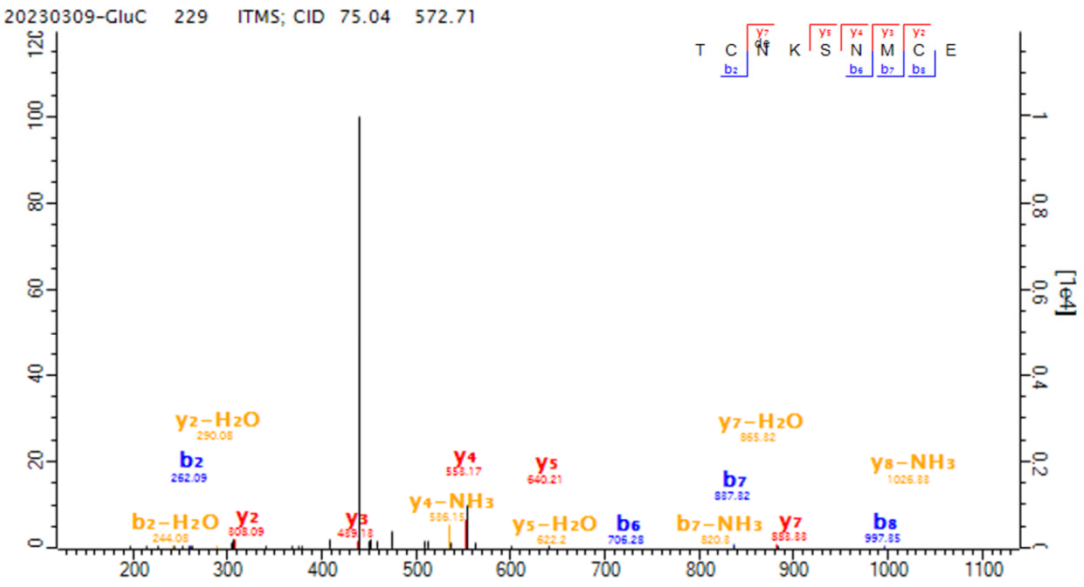

Supplementary Fig. 22 Identification of IL6 Glycopeptides (continued).

c **Without N-glycosylation**

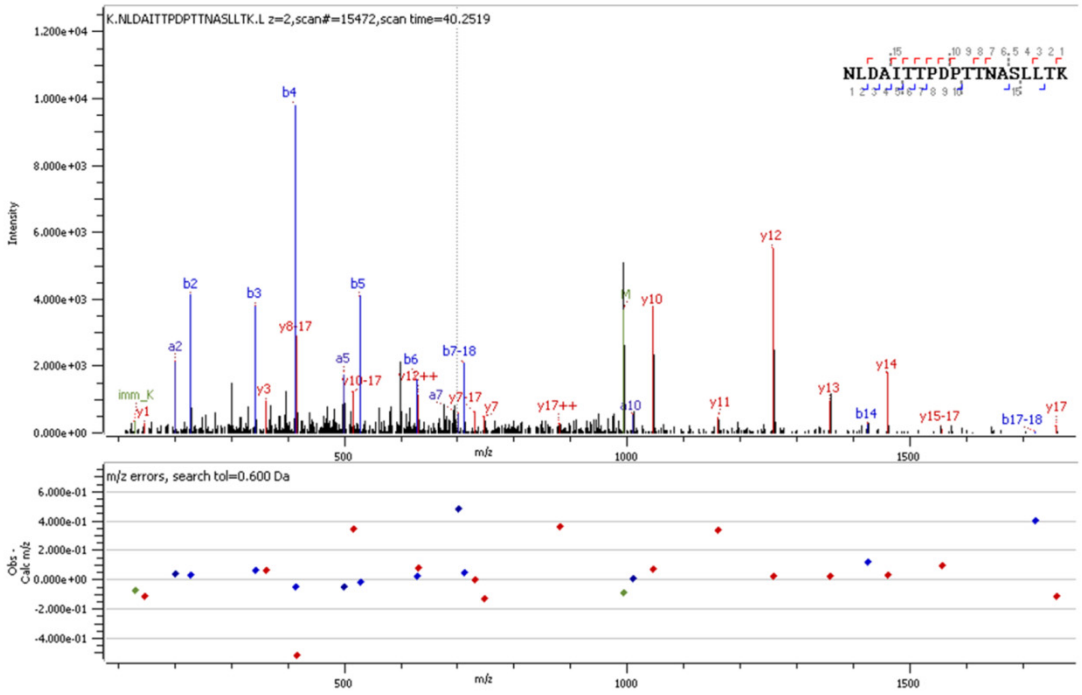

d **With N-glycosylation (N^{172} deamidation)**

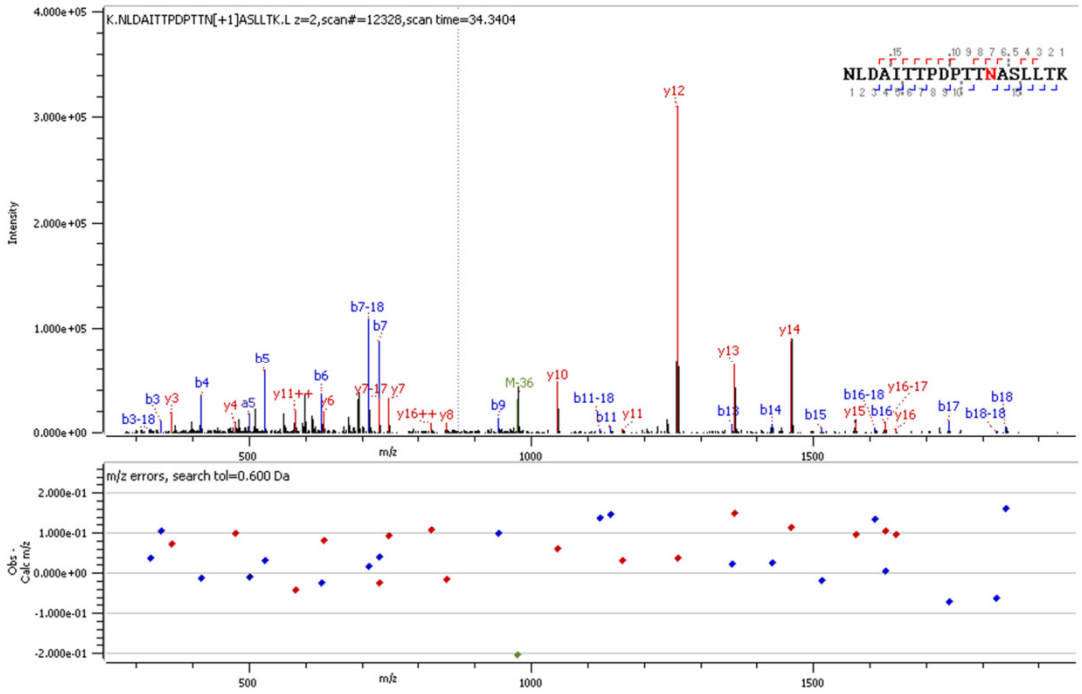

Supplementary Fig. 22 Identification of IL6 Glycopeptides (continued).

e **With O-glycosylation at T170**

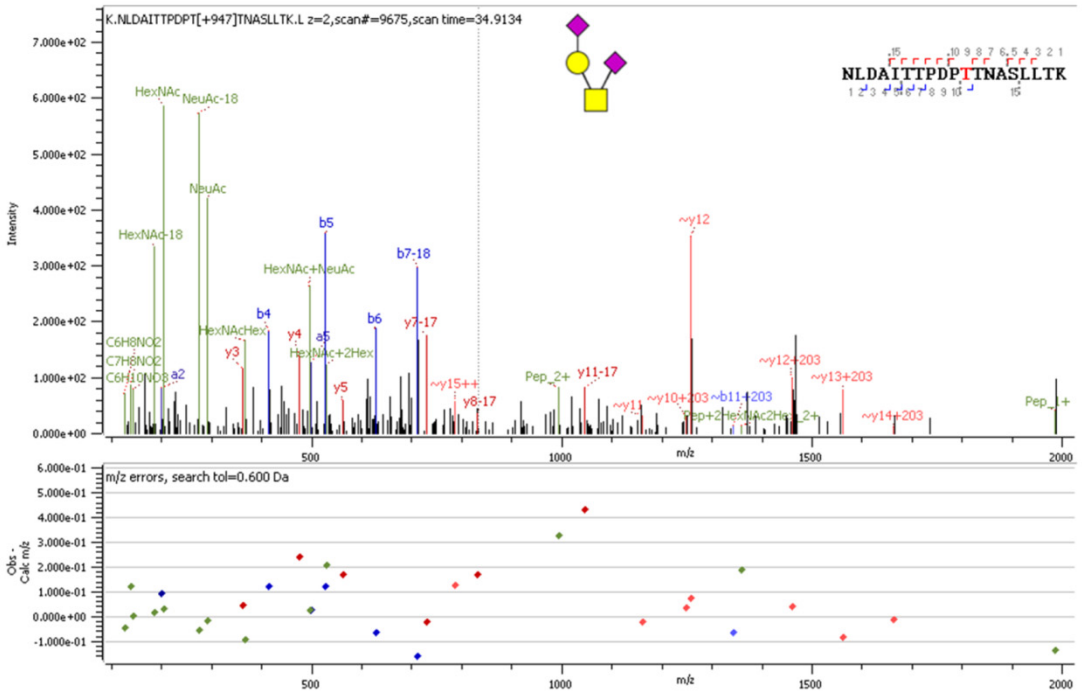

f **With O-glycosylation at T170 and N-glycosylation (N^{172} deamidation)**

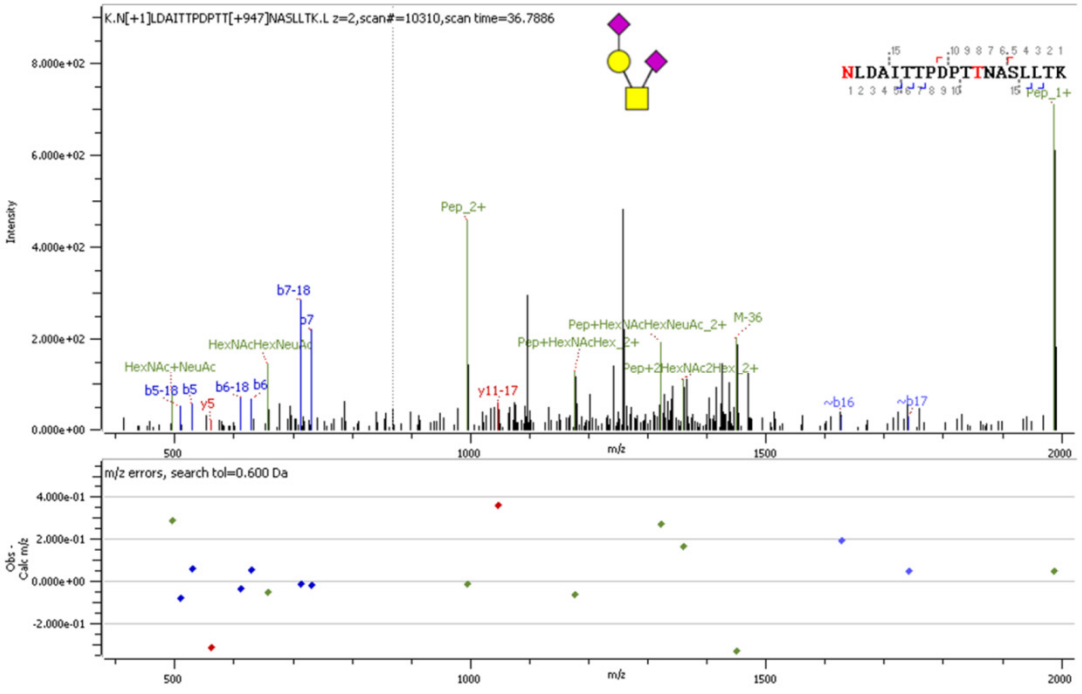

Supplementary Fig. 22 Identification of IL6 Glycopeptides.

(a-b) Identification of the TCN[73]KSNMCE peptide with or without glycosylation.

(c-f) Identification of the NLDAITTPDPT[170]TN[172]ASLLTK peptide with or without glycosylation (**c** and **d**: N172; **e** and **f**: T170).

Supplementary Fig. 23 deNG-IL6 from OR Cells Promotes Cell Migration.

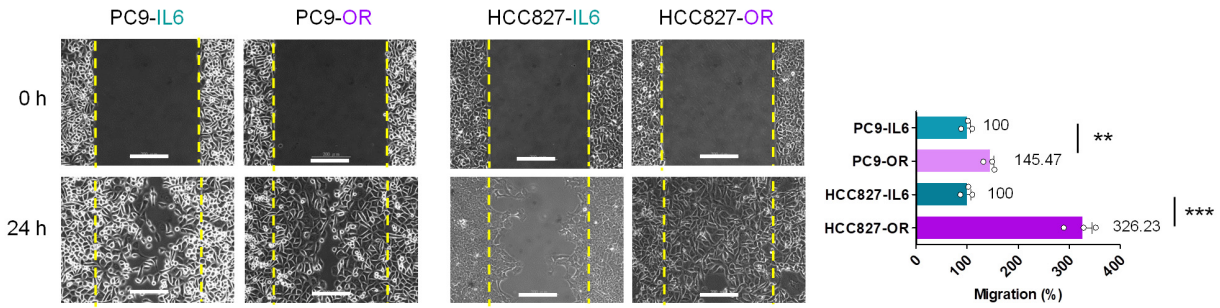

Supplementary Fig. 23 deNG-IL6 from OR Cells Promotes Cell Migration.

Parental and OR PC9 and HCC827 cells were seeded in culture insert and let attached for overnight. Migration of cells through the space made by culture inserts was observed at 0 h and 24 h. The medium contained mitomycin C (5 μg/mL). Scale bars, 200 μm. Quantitative results are next to the images. n=3 independent experiments, mean ± SEM, one-tailed unpaired *t*-test. PC9-IL6 v.s. PC9-OR: **p=0.0080; HCC827-IL6 v.s. HCC827-OR: ***p=0.0003. Source data are provided as a Source Data file.

Supplementary Fig. 24 Treatment History of NSCLC Patients Who Contributed MPE Specimens.

a

EGFR TKI-Naïve Patients	EGFR Status Prior to TKI Treatment	Treatment History
TN-01	Exon 19 del	TKI-naïve
TN-02	Exon 19 del	TKI-naïve
TN-03	Exon 21 L858R	TKI-naïve
TN-04	Exon 21 L858R	TKI-naïve

b

EGFR TKI-Resistant Patients	EGFR Status Prior to TKI Treatment	Somatic T790M	Treatment History	
			First-Line	Second-Line
TR-01	Exon 21 L858R	No	Gefitinib	Osimertinib
TR-02	Exon 19 del	Yes	Erlotinib +Bevacizumab	Osimertinib
TR-03	Exon 19 del	N.D.	Afatinib	Osimertinib
TR-04	Exon 21 L858R	N.D.	Erlotinib +Bevacizumab	Pemetrexed +Carboplatin
TR-05	p.L861Q (CTG>CAG)	Yes	Afatinib	_

Supplementary Fig. 24 Treatment History of NSCLC Patients Who Contributed MPE Specimens.

(a) EGFR status of EGFR TKI-naïve patients.

(b) Treatment history of EGFR-TKI-resistant patients. N.D., not determined.

Supplementary Fig. 25 Characterized Resistance Mechanisms of the LAT Patients.

Patient	Line of Treatment	Resistance mechanisms	Somatic T790M	Paired WES Pre/post	Paired RNA-seq Pre/post
LAT001	First	*CBL*, *KRAS*, *MET* & other amps	No	Yes	Yes
LAT002	First	*MET* amp	No	Post only	No
LAT003	Second	*EGFR* amp & *EGFR* C797S mutation	Yes	Yes	No
LAT005	Second	SCLC transformation	Yes	Post only	No
LAT006	First	*EGFR*, *MET* amp & *TP53* A24fs	No	Yes	Yes
LAT009	First	*TP53* G112V & *CTNNB1* S33C mutations	Germline	Yes	Yes
LAT010	First	Mixed NSCLC & SCLC transformation	No	Yes	Yes
LAT011	Second	Unknown by exome; NE-differentiation without histologic transformation by RNA-seq	Yes	Yes	Yes
LAT014	First	*EGFR*, *KRAS* & *MET* amp	No	Yes	Yes
LAT015	Second	*MET* & other amps & *EGFR* C797S	Yes	Post only	No
LAT016	Second	*AGK*(2) – *BRAF*(8) fusion & *MKRN1*(4) – *BRAF*(11) fusion	Yes	Yes	Yes
LAT017	Second	*EGFR* & *YES1* amp	No	Yes	Yes
LAT021	First	*CD274* (*PD-L1*) & *MET* amp	No	Yes	No
LAT022	First	*EGFR* C797S & *ESR1*(6) – *AKAP12*(4) fusion	No	Yes	Yes
LAT028	First	*EGFR* & *MET* amp	No	Yes	Yes

Acquired and modified from **Roper N, et al.** **Cell Rep Med 1,100007. 2020.** (PMID:32483558)

Supplementary Fig. 26 ssGSEA Enrichment Plot for TFs of N-OST Genes in OR Tumors from Patient LAT017 Before and After Development of Osimertinib Resistance.

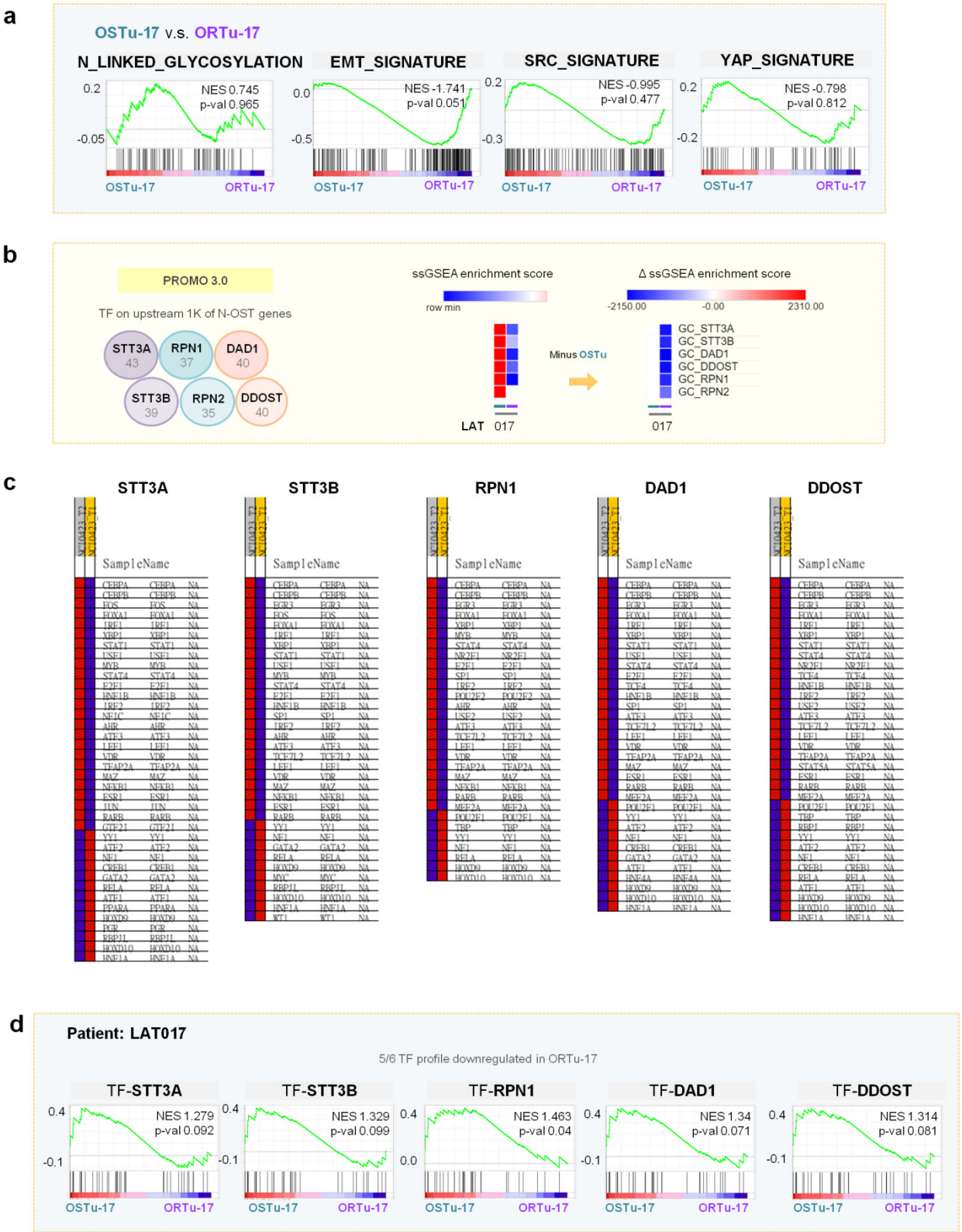

Supplementary Fig. 26 ssGSEA Enrichment Plot for TFs of N-OST Genes in OR Tumors from Patient LAT017 Before and After Osimertinib Resistance.

(a) ssGSEA enrichment plots showing the N-glycosylation, EMT, SRC and YAP signatures in OR tumors from patient LAT017 before and after osimertinib resistance.

(b) Enrichment heatmap showing the TF profile for each N-OST gene in OR tumors from patient LAT017 before and after osimertinib resistance.

(c) Heatmap showing the expression of individual TF genes for each N-OST gene in OR tumors from patient LAT017 before and after osimertinib resistance.

(d) ssGSEA enrichment plot showing the TF profile for each N-OST in OR tumors from patient LAT017 before and after osimertinib resistance.

Supplementary Fig. 27 Treatment History of NSCLC Patients Who Contributed Paired Lung Cancer Tissues.

Patients	EGFR Status Prior to TKI Treatment	Somatic T790M	Treatment	Date of First Biopsy	Date of Rebiopsy
TKI-01	Exon 19 del	Yes	Gefitinib	09/08/2013	20/06/2014
TKI-02	Exon 19 del	Yes	Gefitinib	07/05/2012	07/07/2014
TKI-03	Exon 21 L858R	No	Gefitinib	22/06/2012	11/07/2014
TKI-04	Exon 19 del	Yes	Gefitinib	14/01/2014	05/05/2017
TKI-05	Exon 21 L858R	Yes	Gefitinib	29/09/2016	11/05/2017
TKI-06	Exon 21 L858R	Yes	Gefitinib	13/09/2013	21/06/2017

Supplementary Fig. 28 H&E Staining Images of the Paired TKI-Naïve and TKI-Resistant NSCLC Tissues.

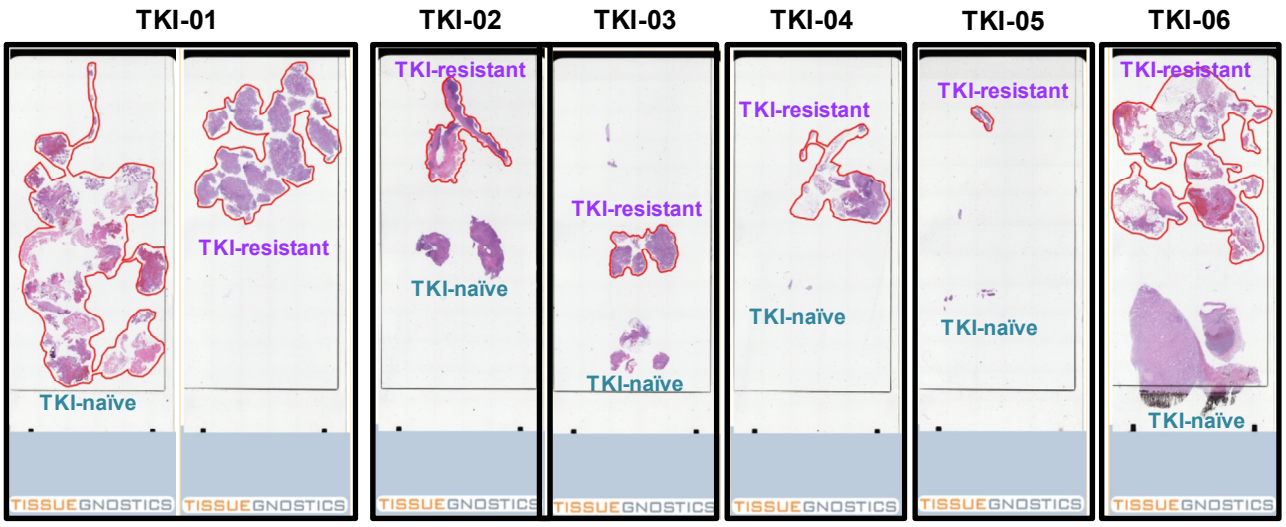

Supplementary Fig. 28 H&E Staining Images of the Paired TKI-Naïve and TKI-Resistant NSCLC Tissues.

Paired lung cancer tissues from the same NSCLC patient obtained before and after the development of EGFR TKI resistance were attached to a single slide for H&E staining and IF staining (Fig. 8e).